Zachary Taylor

O.P.V. Transportable Power Station

Metropolia University of Applied Sciences

Bachelor of Engineering

Degree Programme

Thesis

19 March 2018

Metropolia

Author Title Number of Pages Date	Zachary Taylor O.P.V. Transportable Power Station 31 pages + 3 appendices 19 March 2018
Degree	Bachelor of Engineering
Degree Programme	Environmental Engineering
Professional Major	Renewable Energy Engineering
Instructors	Kari Salmi, Principal Lecturer

In this thesis the CAD design and Circuit Diagrams of a transportable, clean, and renewable public power station made of organic photovoltaics (OPV) is presented and explained. OPV is a liquid carbon-based solar energy production material that can be inexpensively printed into many sizes and shapes on either glass or flexible plastic substrates.

It has been modelled in the vein of outdoor open-air sun-shade flexible umbrellas popularly used in areas such as outdoor restaurant seating, picnic tables in parks, and similar outdoor business functions. It contains LED lighting within the arm framework to provide clean, renewable, and free lighting to outdoor public areas, as well as a single USB charging station, all connected to a central battery bank charged throughout the day by the OPV material that makes up the Umbrella.

The fundamentals of OPV are discussed, the design of the device is presented and explained, the calculations for theoretical power output are shown and discuss based on the design dimensions. All done in the hopes of sparking interest in much needed further research that would allow a final fully realized prototype to be created.

Keywords	photovoltaic, organic, solar, umbrella, charging station, LED

Contents

List of Abbreviations

CAD	Computer Aided Design.
eV	Electron-volts
ETL	Electron Transfer Layer
FF	Fill Factor, the ratio of the open-circuit voltage and the short-circuit current to the maximum obtainable power
HTL	Hole Transfer Layer
J_SC	Short-Circuit Current, the maximum current a circuit can produce, occurs when the circuit is short-circuited as the name implies
LED	Light Emitting Diode
OPV	organic photovoltaic (Any carbon-based material that produces the Photovoltaic Effect)
USB	Universal Serial Bus
R_S	Series Resistance
R_SA	Resistive Power Loss
R_SH	Shunt Resistance
V_OC	Open-Circuit Voltage, the maximum voltage a circuit can produce, occurs when there is no load.

1 Introduction

One of the most common problems with any emerging technology or material is the creation, development, and implementation of practical applications. This is difficult for any number of reasons, the least of which being the sheer number of ideas and the lack of knowledge about their viability combined with the impossibility of committing time to them all. Thus, the responsibility must be shared to allow what would be impossible alone, to be overcome together. That is the purpose of this thesis, to take the opportunities provided by a new technology and explore just one out of the numerous possible applications.

This technology is called organic photovoltaics (OPV) and is a way of producing the photovoltaic Effect in a carbon-based material that is economically viable based on its low production cost in comparison to traditional silicon based photovoltaic materials. Aside from its production cost, the most obvious and useful advantages of this material is its flexibility and light weight. Traditional silicon cells (wafers) are extremely fragile and brittle, and therefore require expensive and/or heavy environmental shielding. This reduces the possible applications of these cells down to rigid structures.

With that in mind, this application seeks to take advantage of a photovoltaic material that is both lightweight and flexible to create a portable power station that can be implemented into widespread daily life, replacing both a common contraption and fulfilling a need all with one device.

The Sun-Brella, as it is affectionately referred to, is such an application. It has been designed to replace standard outdoor seating area umbrellas that serve both to provide shade and shelter from adverse weather. With its larger structure it is directly useful in outdoor business functions, restaurant seating areas, and the like. The cells themselves charge batteries, which power LED lighting on the frame to provide free and clean lighting once the sun goes down and has a USB charging station to allow those taking advantage of this device to charge their mobile devices.

This thesis will display and discuss the design of such a device in the hopes of providing a framework for further study into it viability, as much more study is needed, and additional real-world applications.

2 Theoretical Background

The origins of organic materials that produce the photovoltaic Effect go back a long way and is rooted deeply in organic chemistry, starting with the observation of photoconductivity in solid anthracene in the back in the early days of the 19th century [2, p.1]. However, the ability to have a material that produces this effect reliably, sustainably, and at an amount that can be useful for modern electronics is a more recent around the 1950's when major breakthroughs in the technology by Dr. Ching W. Tang allowed for a conversion efficiency of ~1%, which was significantly beyond the previous <0.1%.[2, p.1]

There is a basic working principle that all materials that produce electricity from sunlight are based on, the photovoltaic Effect. This, in brief, is the effect that when an electron is given a packet of energy (normally in the form of a photon) sufficient enough it will jump from the valence band in which it resides up to the conductive band of said atom, the conductive band being an orbital that allows the electron to move freely about the material. The amount of energy required varies wildly based on the material, as shown in Figure 1 with 3 variations, and its properties and is referred to as its band gap, and in all photovoltaic material is the amount of energy that can be delivered by a photon, meaning the electron movement can be induced by light of an appropriate wavelength matching the eV (electron volts) required for the jump. [7, p.3]

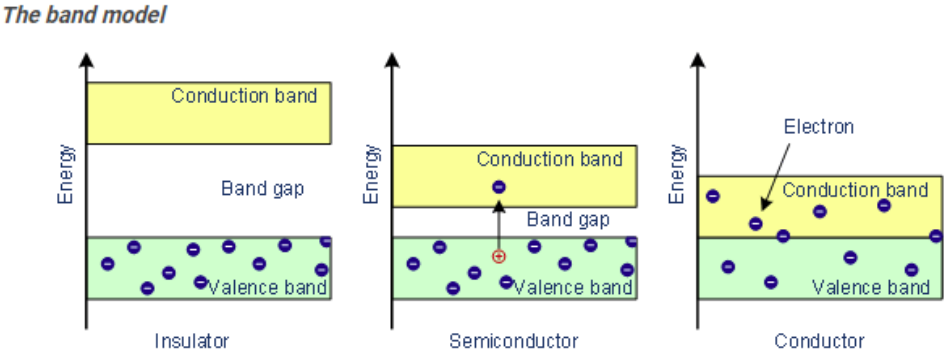

Figure 1 - The Band Model (HB) [7, p. 5]

Once the electron has been displaced up to the conductive band, it leaves behind a “hole”, or more precisely the negative charge is extracted leaving behind an equal positive charge. [3, p. 1]

To make use of this, a standard photovoltaic material needs to have many layers. These traditionally are referred to as the p and n type layers, commonly referred to as donor and acceptor materials, and the p-n junction (Figure 2).

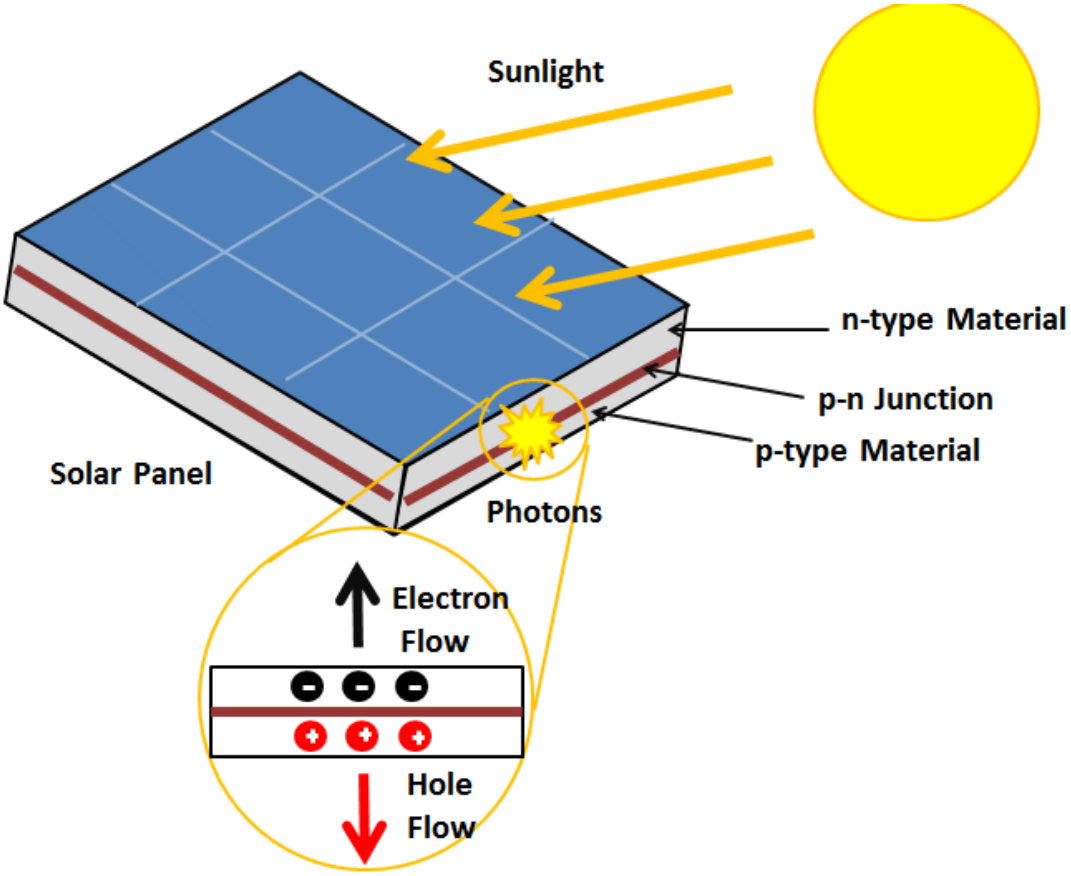

Figure 2 - Photovoltaic Effect (PE) [3, p.1]

The both types of materials are doped, meaning to merge them with alternative materials to add/remove properties, to make the n-type material contain additional electrons and the p-type materials to contain additional holes. In standard silicon solar cells this is achieved by doping the silicon semi-conduction with boron to achieve additional holes, and phosphorous to achieve additional electrons. [8, p. 6]

With these layers and the junctions put together, when the sunlight strikes the n-type material, its sets lose the previously explained electron and hole pair, referred to as an *exciton*. Due to an electric field caused by the p-n junction, the exciton’s two constituent pieces move opposite to

what one would expect them to and move about the material, it is this movement and its resulting effects on the material that cause the electrical current to be produced.

With the basics understood, OPV materials producing an electric current are not significantly different. The only major differences, within the scope of this thesis of course, are what the p and n type materials are made from. Instead of using a silicon semi-conductor and doping it with other minerals, organic chemistry instead is used.

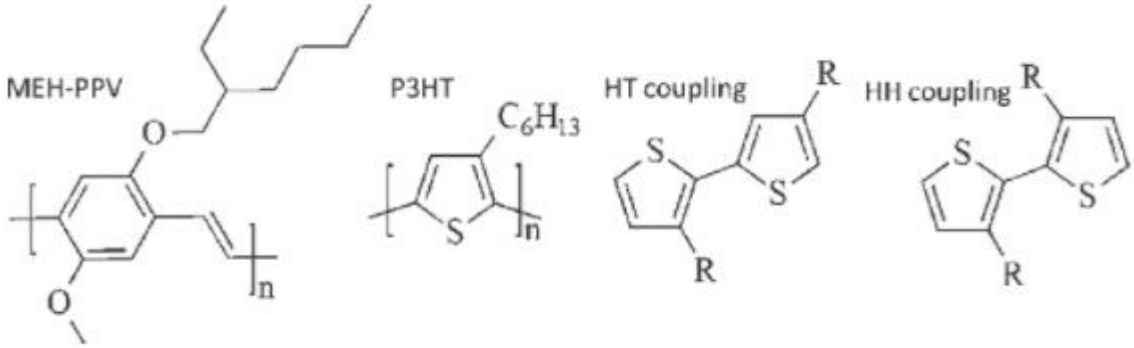

Figure 3 - Common Donor Materials (ML) [5, p. 8]

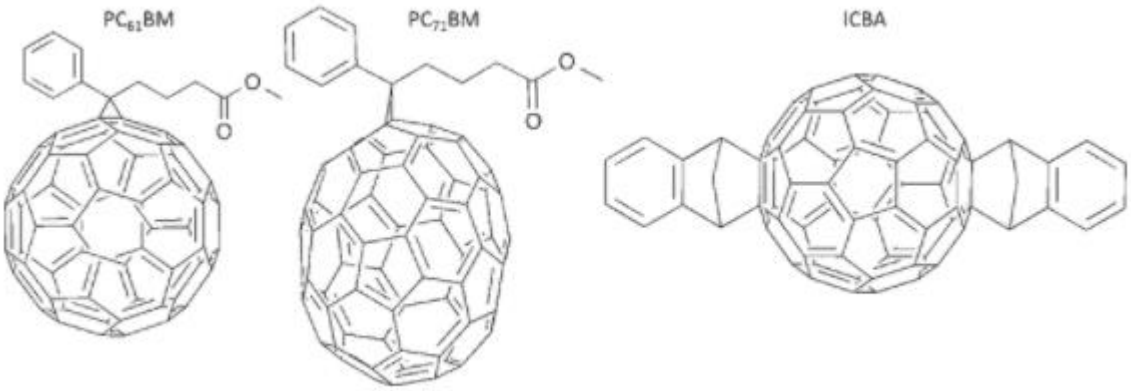

Figure 4 - Common Acceptor Materials (ML) [5, p.9]

In Figures 3 and 4 some common donor and acceptor materials are shown; these can vary depending on need. Figure 5 is an illustration of the photovoltaic effect as it occurs within OPV materials.

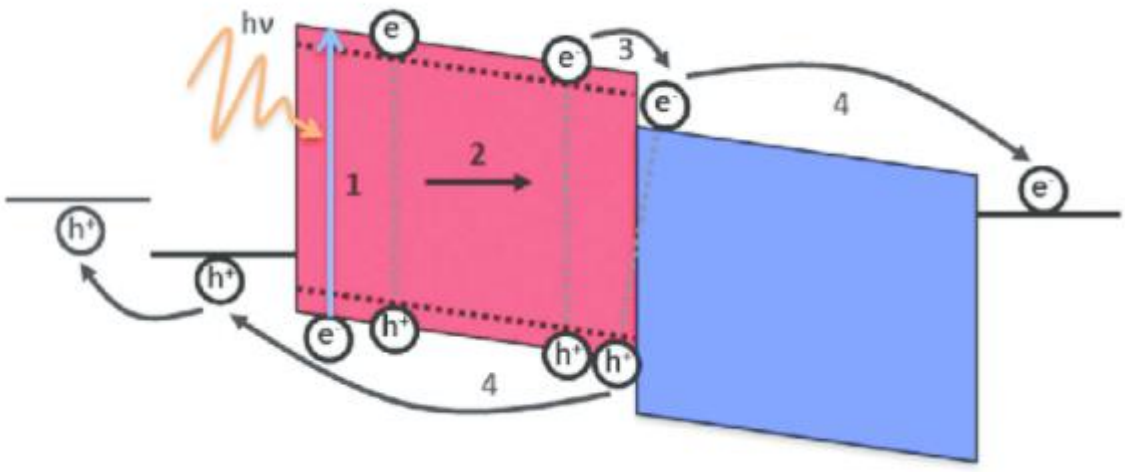

Figure 5 - Acceptor/Donor Example (ML) [5, p.4]

With e- of course being a symbol for the negatively charged electron, and h+ being a symbol for the positively charged *hole*, and *hv* modeling its *band gap* energy required to initiate the movement of the exciton.

Now in reality, this reaction occurs all over the cell; this is because one major difference between traditional silicon solar cells and OPV that should be understood is how the layers interact. As shown in Figure 2, silicon is layer upon layer, however OPV materials use a process called bulk heterojunction configuration, which is the mixing of the donor and acceptor layers into one single layer to allow for better reception of the loose excitons, as seen in Figure 6. [4, p.24]

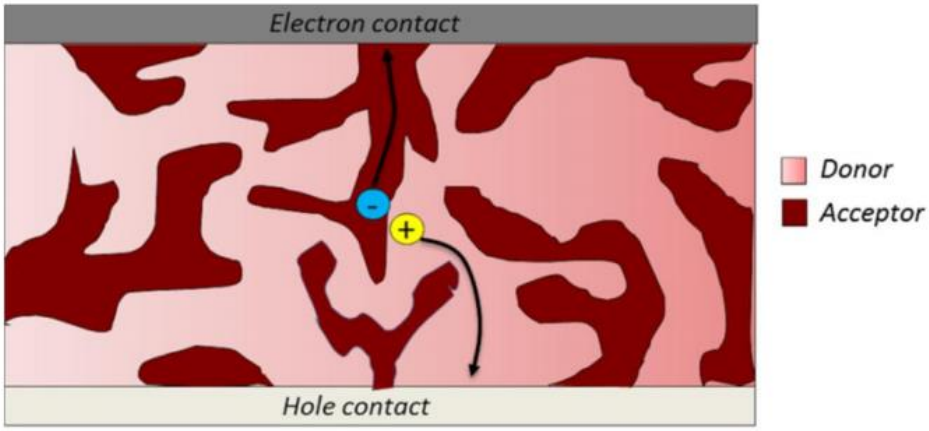

Figure 6 - Heterojunction Example (PA) [4, p. 24]

Once the junction layer in complete, the cell itself then consists of a series of layers to allow the exciton's constituents to travel and connect to further conductive substrates to allow it to be connected to electronic systems.

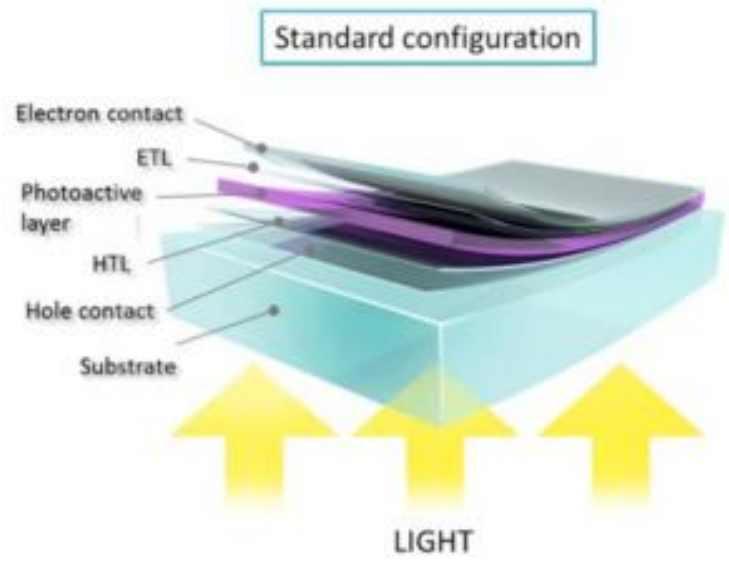

Figure 7 – Basic OPV Layer configuration (PA) [4, p. 28]

As shown in Figure 7, the light comes in and interacts with the photoactive layer, with sets off the movement of the exciton. Due to the previously mentioned electronic field, the electron is repelled and connects with the ETL, electron transfer layer, and the hole interacts with the HTL, hole transfer layer, both of which then connect with their own conductive contact and create the desired current. [4, p. 28]

The substrate of Figure 7, or any OPV, can consist normally of any transparent material such as glass or plastic. This is the most significant advantage, regarding this thesis, that OPV has over the traditional silicon solar cell. It can be attached to a flexible substrate such as plastic (Figure 8).

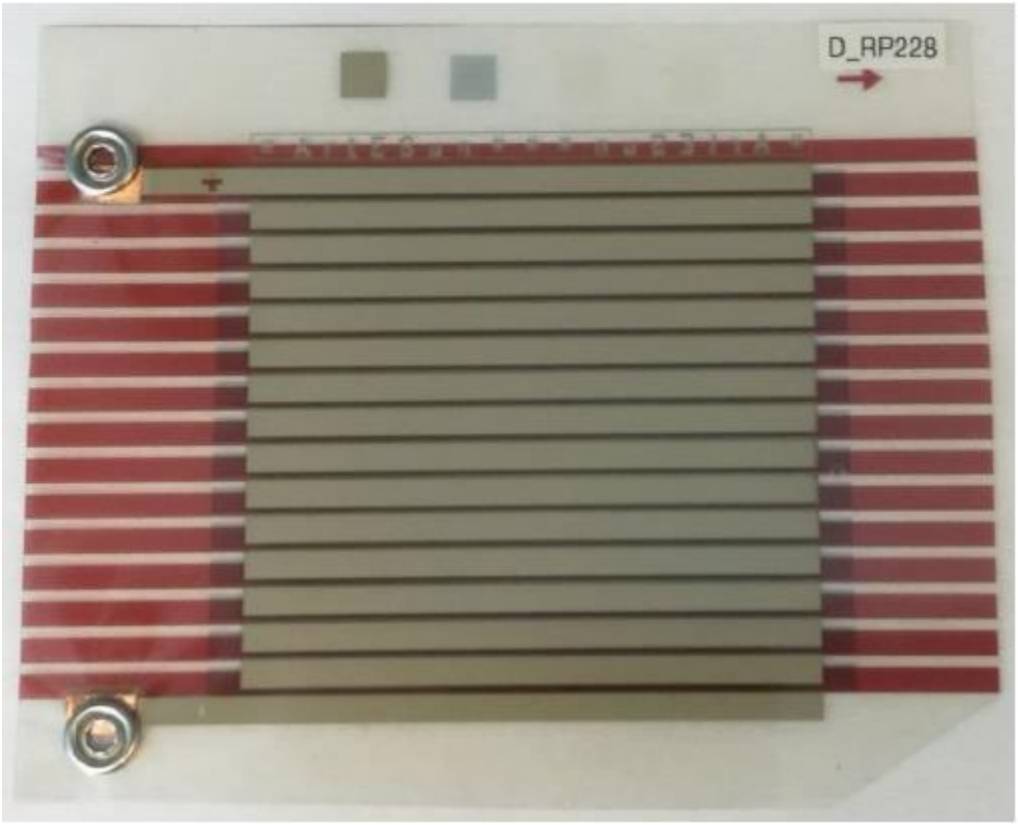

Figure 8 – Yrjänä, S. (2017). Modules to Metropolia 6/2017 [Image]. Retrieved from LIWE Facades Project by Metropolia U.A.S.

This is a “game-changer” regarding how it can be implemented. Traditionally, solar cells are extremely rigid and fragile due to the silicon itself and that the cells are produced extremely thinly since only the top layers are needed and waste is discouraged. This drastically limits how they can be used since they require sizable environmental shielding which is rigid and heavy. Not so with OPV, as with a thin plastic substrate they can be used in a much wider variety of functions.

All of this considered, what occurs is that each cell, or collection of a specific area of photovoltaic material with an additionally connected conductive substrate, is that it becomes a current source for any electrical circuit.

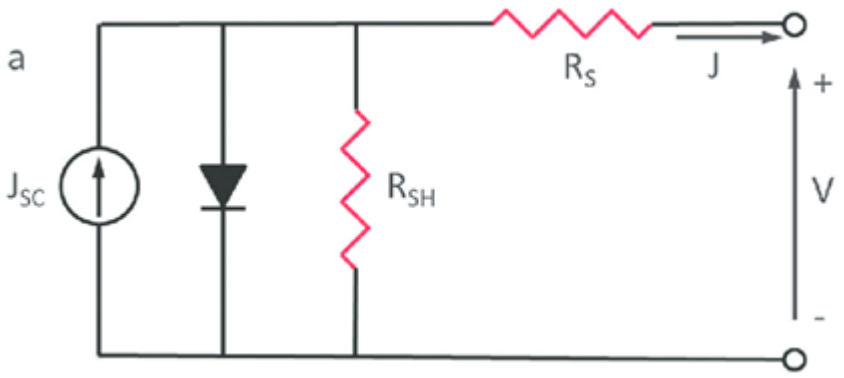

Figure 9 - Equivalent Circuit Model (ML) [5, p.5]

As shown in Figure 9, this is the equivalent circuit model of what occurs within the OPV cells itself. J_SC is a value referred to as *short-circuit current* which is the maximum possible current a circuit can produce. The  being a diode, or a one-way path for any electrical current. And R_S and R_SH being the series and shunt resistance respectively, which models the internal electrical resistance of the material and circuit itself. [5, p. 5]

Another major difference between silicon solar cells and OPV is the production. This is another advantage that this thesis tries to take advantage of, and an overall advantage for OPV in general. Where silicon solar cells are produced mainly through a process when silicon ingots are grown in large crystals to insure high purity called the Czochralski process, OPV materials can be printed in a roll-to-roll printing process that is both less time consuming and significantly less expensive. There are two main ways of printing OPV, gravure printing and metal aerosol jet printing. Both have their advantages and disadvantages and will be explained briefly.

Gravure printing is where two cylinders are rolled together with the bottom cylinder immersed into the “ink” (or in this case the OPV material) and the top cylinder creates whatever impression is desired, as seen in Figure 10. Some advantages are the simplicity in technique; however, a disadvantage is the initial cost of each cylinder can be prohibitive. [4, p. 32]

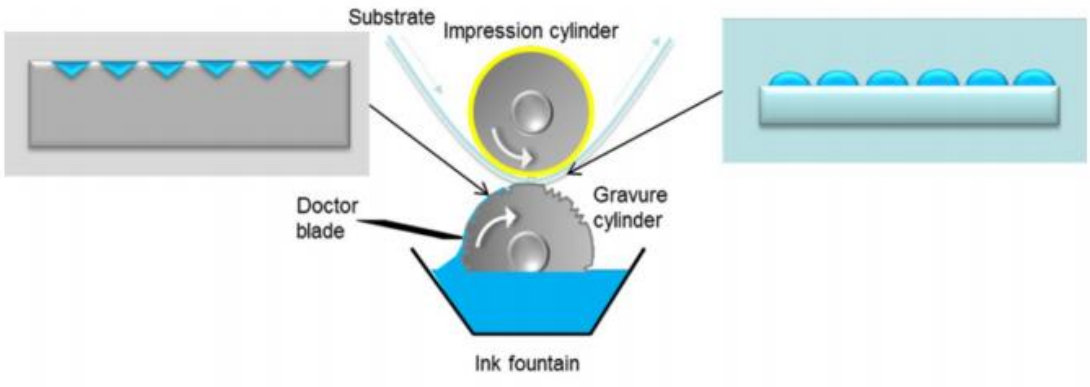

Figure 10 - Granure Printing (PA) [4, p. 32]

Metal aerosol jet printing is the method where the *ink* is turned into an aerosol, normally using ultra-sonic methods, which is then sprayed onto the substrate, as seen in Figure 11. An advantage of this is it is a *non-contact* printing method and the ink properties are not so tightly limited; however, some disadvantages include higher cost and slower production speeds. [4, p. 35-36]

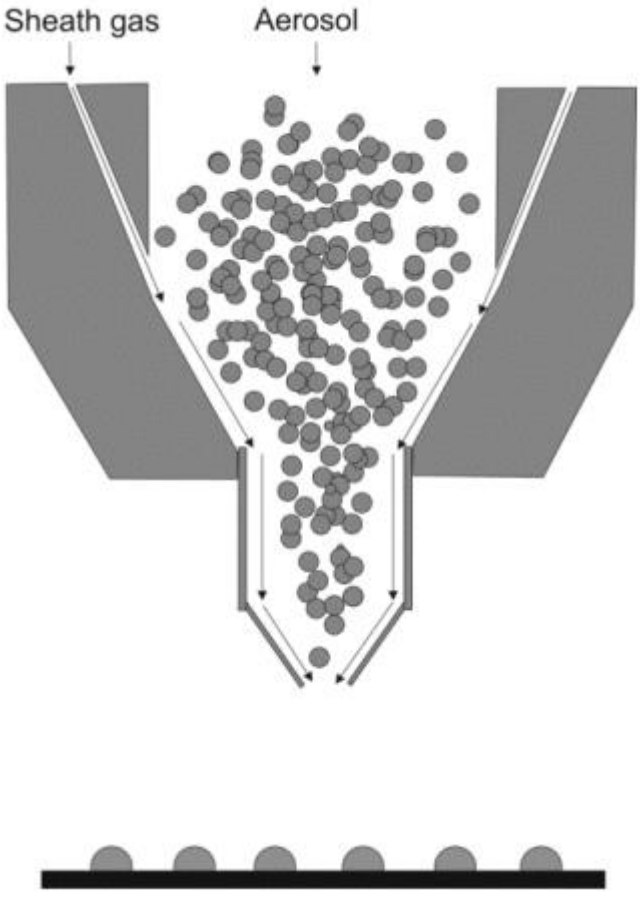

Figure 11 - Metal Aerosol Jet Printing (PA) [4, p. 36]

With an understanding of how OPV materials work, and an equivalent circuit model that allows computer modelling of this material, it is time to move on to the creation of a device that uses this knowledge to model larger scale OPV panels and CAD designs of devices used to manage and harness the electrical currents produced.

3 Methods and Materials

The material in question for this thesis was created and produced by a team working out of the Finnish research institute VTT (http://www.vttresearch.com/), headed by Research Team Leader Tapio Ritvonen and Senior Scientist Marja Välimäki, with the main personal contact for this project being Samuli Yrjänä.

Originally the material was provided from VTT to Metropolia University of Applied Science along with a grant from the Finnish funding agency Tekes (www.Tekes.fi). This project was created to take this material and subject it to real-world environmental conditions, as well as physical stress test, and to gather and analyze its production data over the course of several years.

3.1 Materials

For this thesis, the entirety of the works has been done digitally for the purposes of the reduction in cost and the availability of modification without incurring additional cost and minimal time. This allowed 4 separate iterations of the device, each being improved upon the last, without the waste incurred by building each one physically.

The CAD design was completed on Autodesk Inventor Professional 2018 and the Circuit Diagrams completed on National Instruments Multisim 14.1 Student Edition.

3.2 Method

With the basics in hand, the equivalent circuit will be the base structure for the O.P.V. sheets that together will form the Umbrella surface itself. The J_sc of the cell is based on the equivalent cell provided by VTT with the effective area of 80 mm x 85 mm, and considering each of the cell

areas as it progresses down the sheet gets increasingly large, the calculations will be prepared as a multiple of this base dimension, for which the OPV Sheet has been designed so that Row 1 equals the base dimension.
For example, the second row has the dimensions of 116mm x 85mm (all 10 rows are a height of 85 mm) and thus the final current production will be calculated and modeled as: 116/80 = 1.45 so it will be Row 2_Current = 1.45(Row1_Current) and so on.

3.3 CAD

The following section presents the drawings of a completed 3D CAD design of the entire Sun-Brella system done on Autodesk Inventor. The section will begin with the design, and the diverge into a small section for the upper arm and the O.P.V. wing parts as they will require some explanation. Only the drawings relevant to a basic understanding of the system have been included in this section, the drawings can be found in *Appendix 1. CAD Drawings – Sun-Brella Assembly* and *Parts List and Appendix 2. CAD Drawings – Individual Parts*.

The design file itself contains the entirety of the circuitry; however, for one reason or another unknown to the author, this circuitry does not render within the drawings so must be understood from the circuit diagrams discussed in future chapters.

3.3.1 Sun-Brella

Figure 12 (below) is an overall look at the Sun-Brella. The dimensions have been added, aside from obvious reasons, to give an idea of the general size of the structure.

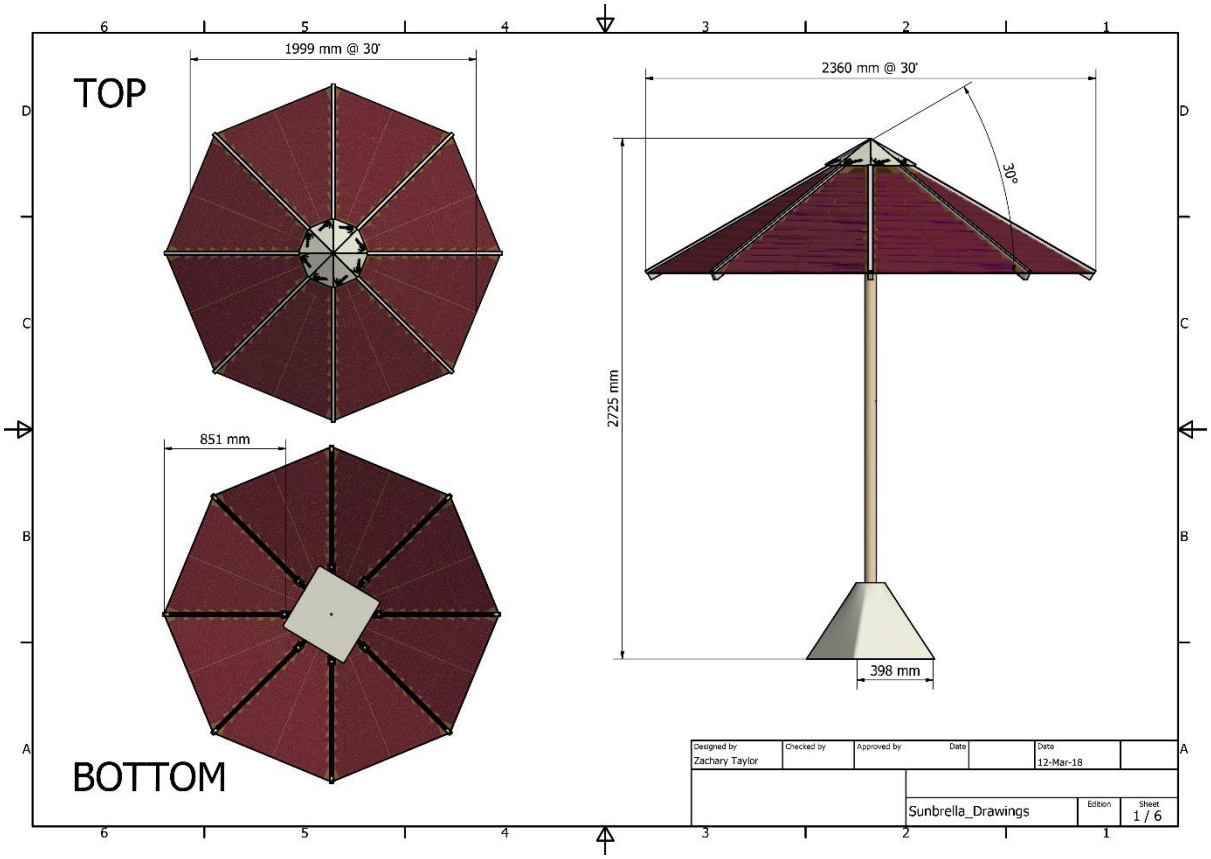

Figure 12 - Sun-Brella Main View

As with most parts of the Sun-Brella, the general dimensions themselves are subject to change due to, for example, possible stresses or needs within the printing technique, weight issues, arm printing issues. These dimensions were chosen to most closely resemble a standard outdoor seating umbrella to continue in the desire to allow the Sun-Brella to slide into a niche already formed by previous technology, again allowing a significantly easier adaptation. This includes the standardization of both the height and the width.

To discuss the design choices, the octagonal shape of the umbrella was chosen over a more traditional hexagon for several reasons. The first of which being that were only 6 sides chosen the amount of dip that each panel would experience in the center due to wider spacing of the support structure would have negatively affected the irradiance levels of each panel. How much

it would have affected it would be something that requires further study, but it is significant at this time.

The fully open angle of 30 degrees was chosen as the best compromise between several factors: sunlight incident angle, shaded area, clearance height of panels, and element protection in undesirable weather conditions. The final decision was to design the umbrella at 30 degrees to allow for the best overall incident angle of the highest number of panels over the course of the day, while at the same time providing a significant shaded area, a comfortable clearance height for the panels to prevent non-ergonomic entrance into the shaded area, and standard water/weather protection in wet conditions.

In future versions the pole will come equipped with tilt angle features, thus allowing a much greater adjustment of angles to optimize the desired service depending on the need at the time.

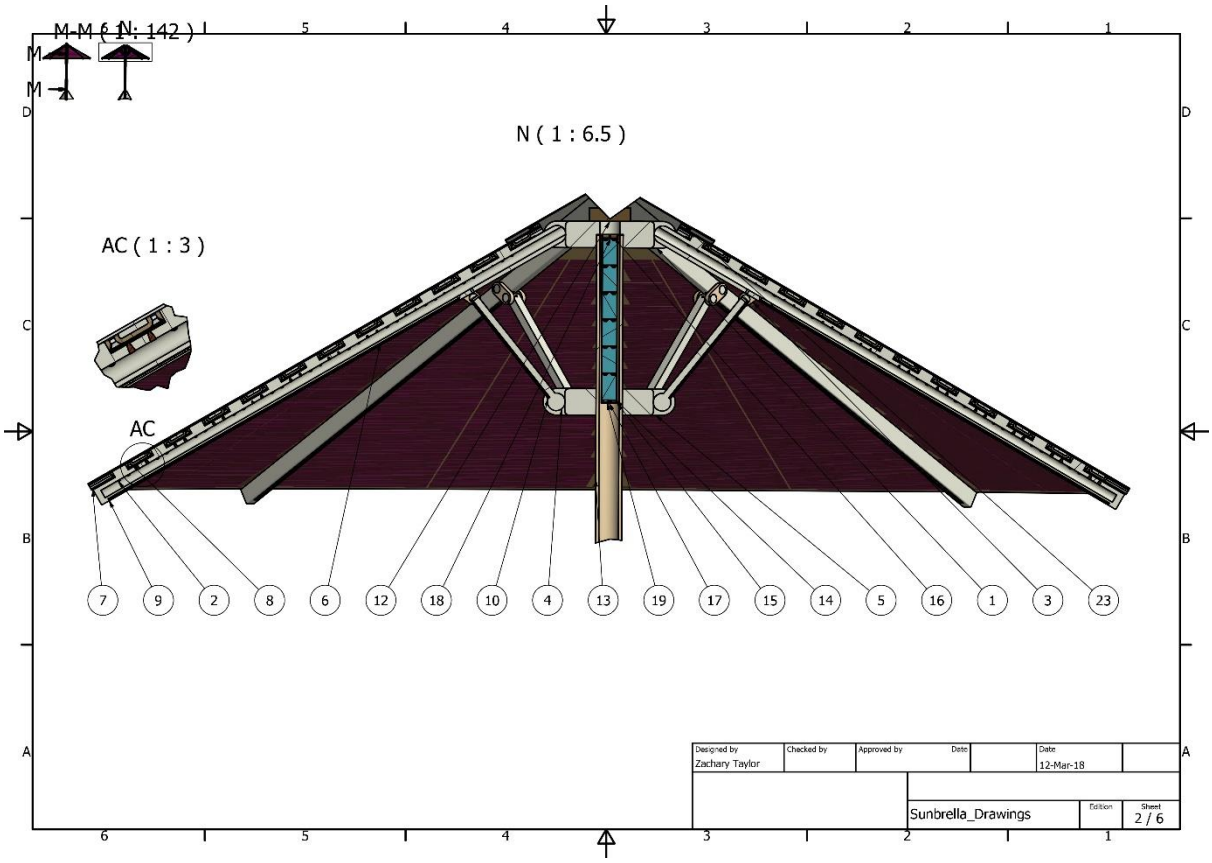

Figure 13 - Sun-Brella Top Cut View

The internal workings of the Sun-Brella rely heavily on each of the 8 upper arm pieces (Part 2) to do most of the work, which will be discussed in further detail in later chapters and a Parts List for each Part Number can be found in Appendix 1. To explain briefly, each arm is hollow with 20 pairs (10 for each panel) of cylindrical positive and negative terminals running down the center, each of which being connected to a corresponding cell within an OPV wing (Part 7). The

underside of each arm, both upper (Part 2) and lower (Part 4), have LED strips (Part 6) that also have all the electrical wiring running up the central hollow of the arm.

Each arm also has clips on the top for the environmental shielding for each terminal (Arm Sheath, Part 8) and to waterproof both the OPV connections and the Sun-Brella's underside. This sheath runs the length of the panels connecting to the Cover (Part 23) that provides the environmental protection for the wiring and charge controller based on top of the upper octagon (Part 1). This sheath serves as both protection and as the clip to keep the OPV wing (Part 7) connected to both the terminals and the arm itself.

After the wiring from all 8 arms are connected, they are run through the charge controller (Part 12) on the top of the upper octagon (Part 1) which is connected to the battery bank (Parts 15-19) situated in the central pole. The wiring for the LEDs (Part 6) are also run through this section but do not connect to charge controller but rather run parallel to it and connect directly to the battery bank (Parts 15-19)

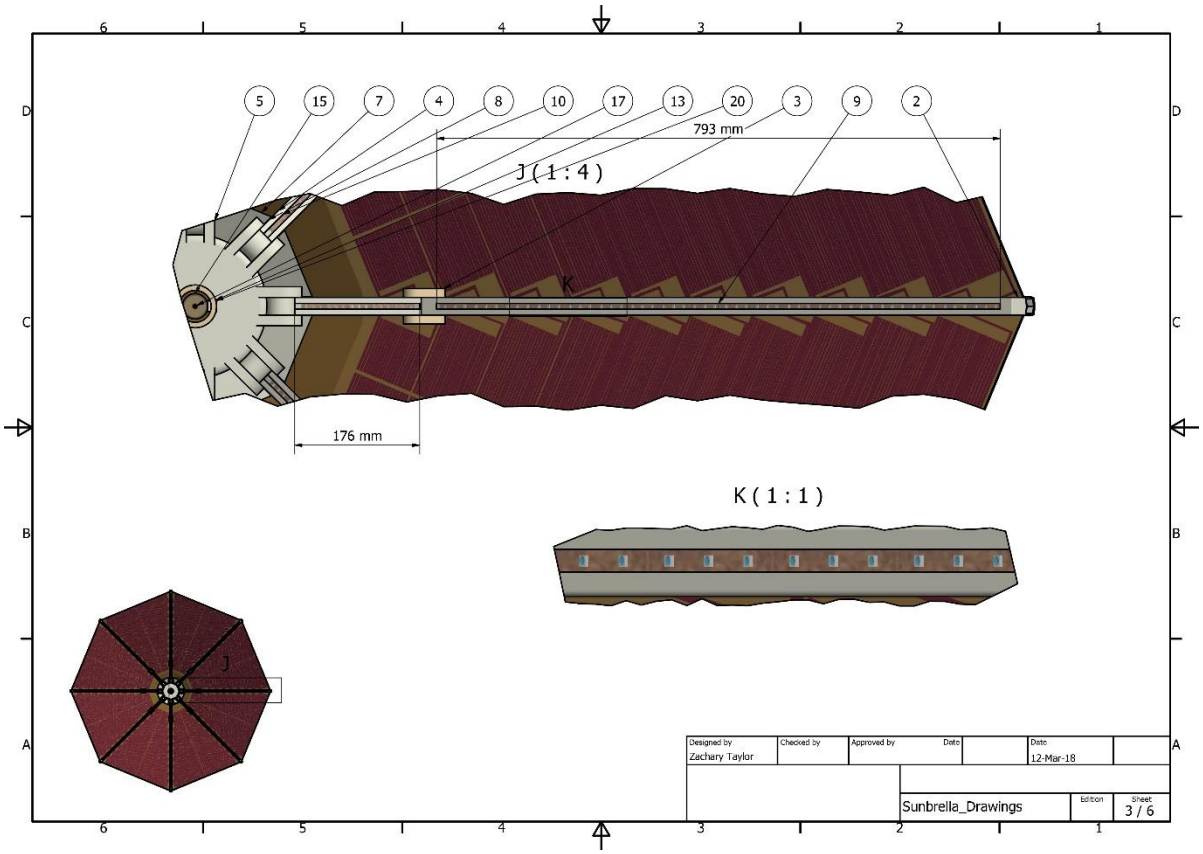

Figure 14 - Sun-Brella Under Arm View

This underside view, Figure 14, shows the attachment of the LED strip into the recess on both the upper and lower arm sections. Both strips are environmentally shielded by a clear plastic

(Parts 9-10) to allow them to illuminate without concern of damage due to exposure to moisture. The wiring for each also runs through small holes within each arm, allowing a full circuit wiring without concern of exposed wires and all the wear and tear issues that come along with that. For further information regarding the recessed sections or travel hole sizes and locations for the wiring the full design drawing for each part can be found in Appendix I.

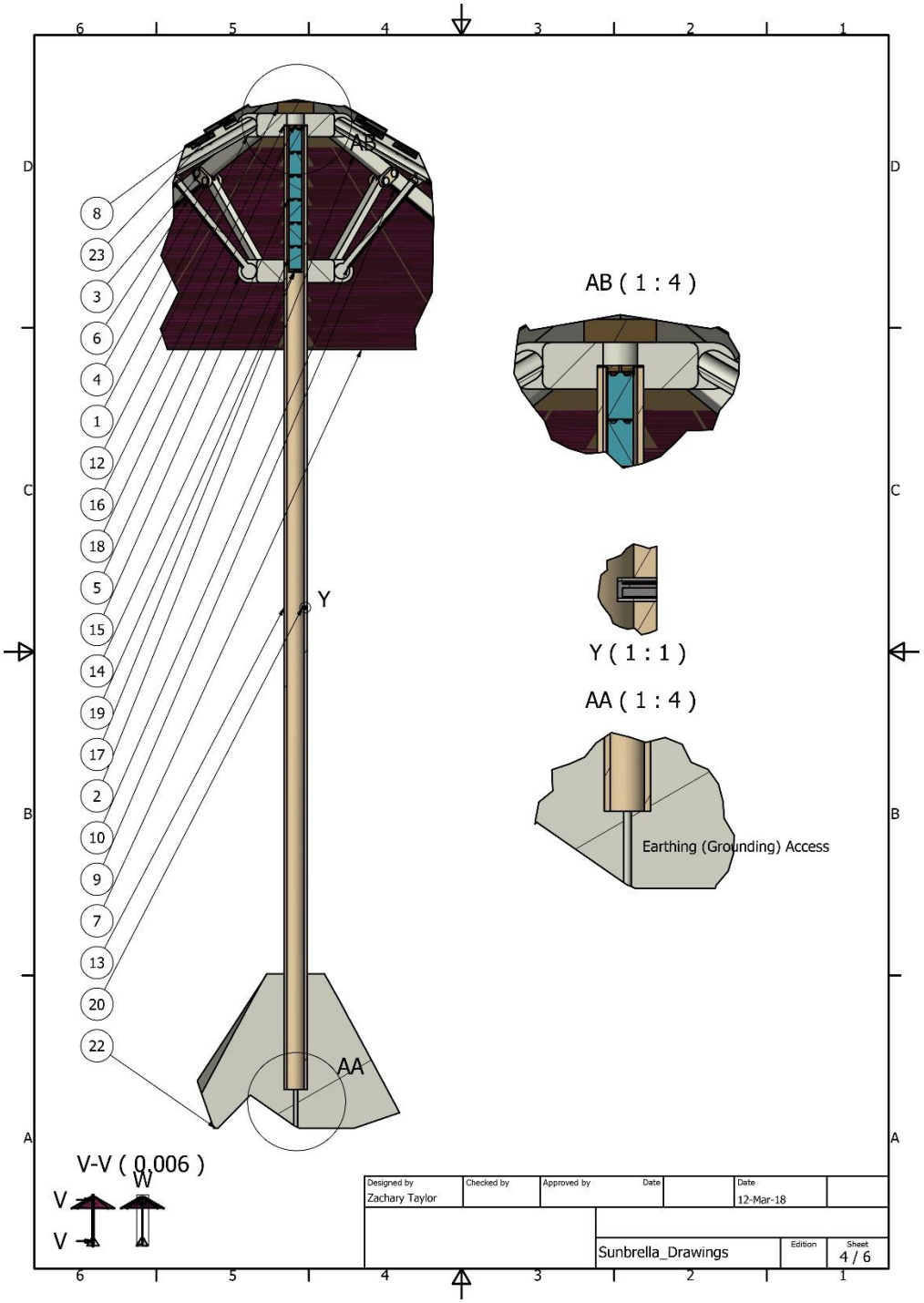

Figure 15 - Sun-Brella Pole Cut View

Continuing past the panels and upper octagon, the lower octagon provides the physical support structure of the arms themselves. They do not, however, contain any electronics or electrical wiring at all. This is quite intentional, as this is the part of the umbrella that will see the single most contact with consumers or users of this device, as well as the most day to day movement up and down the pole. In the same vein of preventing as much damage from exposed wires or natural wear and tear from use, this part has been kept simple and free from any expensive or necessary equipment. It will also be firmly secured to the pole at the appropriate angle both above and below the octagon as one of the largest dangers to this device is wind and preventing the bottom octagons ability to move vertically is one of the design steps taken to prevent possible damage. However, the design of the parts that will attach it to its place on the pole have been left for further iterations, this is to allow time for further research in to the optimum solution.

Continuing down the pole at the halfway point is the USB Port (Part 20), it is connected at the moment directly to the battery bank but in future iterations will be connected through an integrated charging PCB. Only USB port has been included since for simplicity it cannot be guaranteed that there will be enough available power.

At the bottom of the Sun-Brella is the customized stand meant to provide physical support for the structure. It has been modified to allow for a possible earthing of the electronics if legally required. Due to the fact there are no metal or conductive parts on the structure of the device beyond the terminals in each arm, earthing is not a requirement. However, the device has been designed to allow for it as legally it may be required for public areas and extra safety measures are never a bad idea.

3.3.2 Individual Parts

Upper Arm:

As mentioned previously, the upper arm requires further explanation as it is central to the working functions of the Sun-Brella and most of the work is indeed done here. In the Figure 16, there is a clearer picture of what is occurring within the arm itself. The central hollowed tube is clearly visible, which is the pathway for all the electrical wiring coming in and out of the arm, as well as provides the structural support for the 20 terminals references previously.

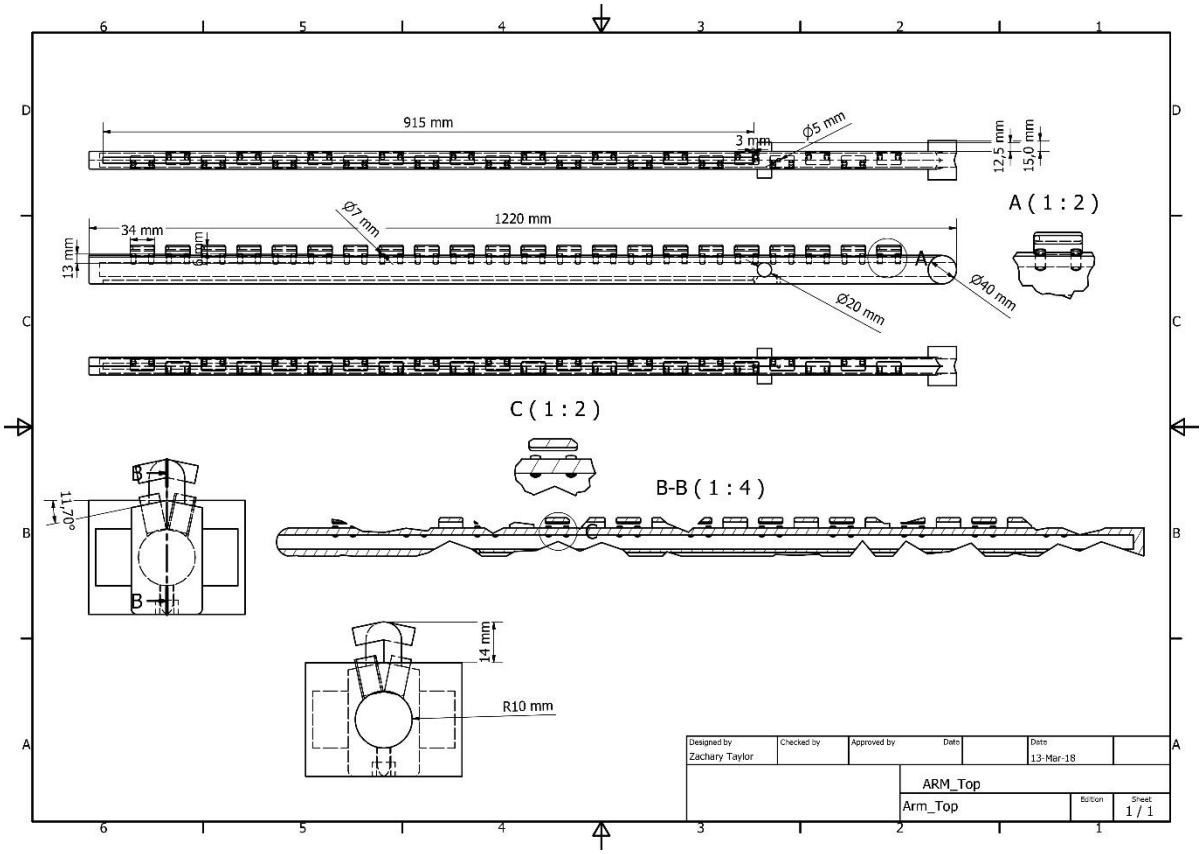

Figure 16 - Upper Arm View

There is now a clearer image of the clips mentioned before, Figure 16, that allow the Arm Sheath to connect and provided the environmental protection and secures the O.P.V. wing to the arm. Having this many connections also allows for greater durability against wind as it spreads out the force placed on the wing over a wide area decreasing potential damage.

One will notice that the main arm with the terminals has been split into two sections and each section has been tilted by 11.7 degrees from center. This has been done very specifically to prevent one of the major sources of wear and tear on the device, the repeated bending of the O.P.V. material. This tilt in the arm allow each arm at 30 degrees to line up horizontally with those immediately to its right and left, thus providing a flat contact surface as a support structure for the wing. The hope is to increase the active lifespan of each wing by limiting the stresses acting upon it. This is also the reason behind having a clip above each of the sets of terminals, spreading the pressure among many points will decrease the amount of stress on each point and hopefully will increase the lifespan of the wing. Further details of the wiring of the arm and wing can be found in the circuit diagram chapter of this thesis.

OPV Wing:

The O.P.V. wing also required further explanation as to its inner workings. It can be seen in Figure 17 that the wing itself is split down the middle into two separate entities.

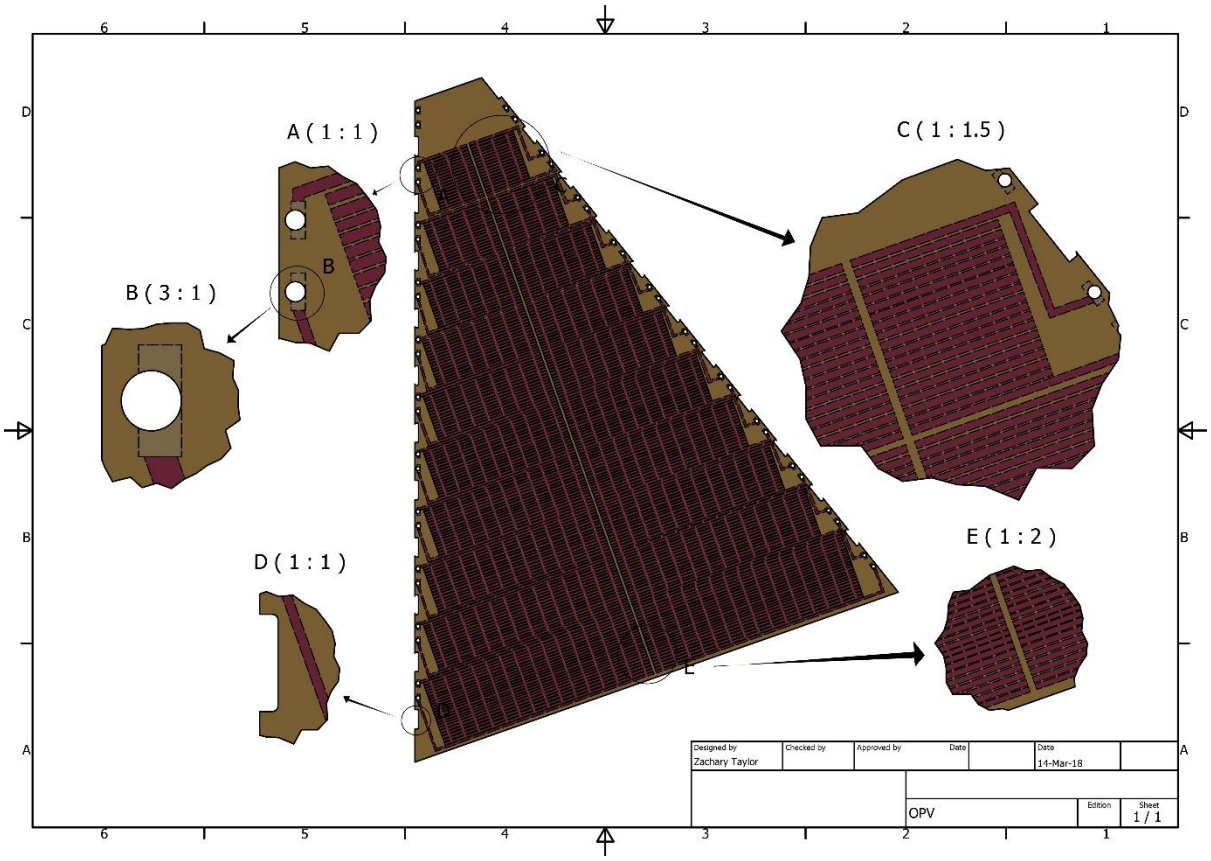

Figure 17 - O.P.V. View

(A: Conductive contact pair, B: One conductive contact, C: Top row to highlight one cell separation, D: Cutout for shield contact, E: Separation of two panels to facilitate bending)

This has been done for a few reasons, the first of which being to decrease the overall length of each individual cell. According to the paper Modelling of Large-Area Solar Cells (2):

> Resistive power losses affect the performance of the solar cell by increasing the series resistance, which is given by rewriting Eq. (2):

$$R_S A = \frac{P_R}{J_{max}^2} \quad (1)$$

> At a given photogenerated current density, the value of *RSA* is proportional to the resistive power losses. Because of the dependence on *L*2 from the ITO component, *RSA* will increase with the length of

the device. It is well known that the series resistance is a parameter which can limit the performance of a solar cell by reducing both *FF* and photocurrent for both inorganic and organic solar cells. (2)

(*R_SA is resistive power loss, L2 is length of substrate, and ITO is indium tin-oxide which is the conductive substrate*)

This meant that it was a goal to keep the area of each cell to a minimum to improve the overall power output. There were many ways to do this; however, finding the balance between loss of functional area due to need for transmission areas or cell separation caused the wing to be designed as it is currently shown. Each descending level of the wing is two separate cells each connected to their own terminal pair, unfortunately by the 10th level of cell the two have gotten rather long and in practice should be an interesting real-world example of the principles discussed in that paper.

The second reason to have the wing divided in two is to accomplish the same goal as so many other design decisions, to reduce the wear and tear of the device over time. The author of this thesis is, at the time of writing, running stress tests on the material itself to see how well its production levels deal with repeated bending, however until that data is known this design will proceed under the assumption that repeated bending of the O.P.V. substrate will cause damage and a significant decrease in production, and thus is to be avoided. Therefore, the printing of this wing is to be sealed in a line down the center to allow for easy folding of the wing when the Sun-Brella is closed, and this line will keep the stress of bending localized to one area that is not essential to production.

Regarding the 20 holes cut out for the corresponding terminals, it can be seen there is a rectangular conductive sheet running around the hole. This is to ensure constant conductive contact between the conductive layer within the wing to the terminal and thus to the wiring, etc. As with the upper arm, for further information regarding the circuitry, please refer to the circuit diagram chapter of this thesis.

3.4 Circuit Diagram

Using the circuit simulator Multisim, a model of the entire Sun-Brella system has been created from the base equivalent circuit on up.

3.4.1 Base Circuit

The base circuit has been modeled after the circuit provided by Mazzio and Luscombe (1). The J_SC has been taken from the data provided by VTT and Samuli Yrjänä; however, the R_S and R_SH are invalid values used merely as a placeholder until the actual value can be measured, so should not be considered valid at this time.

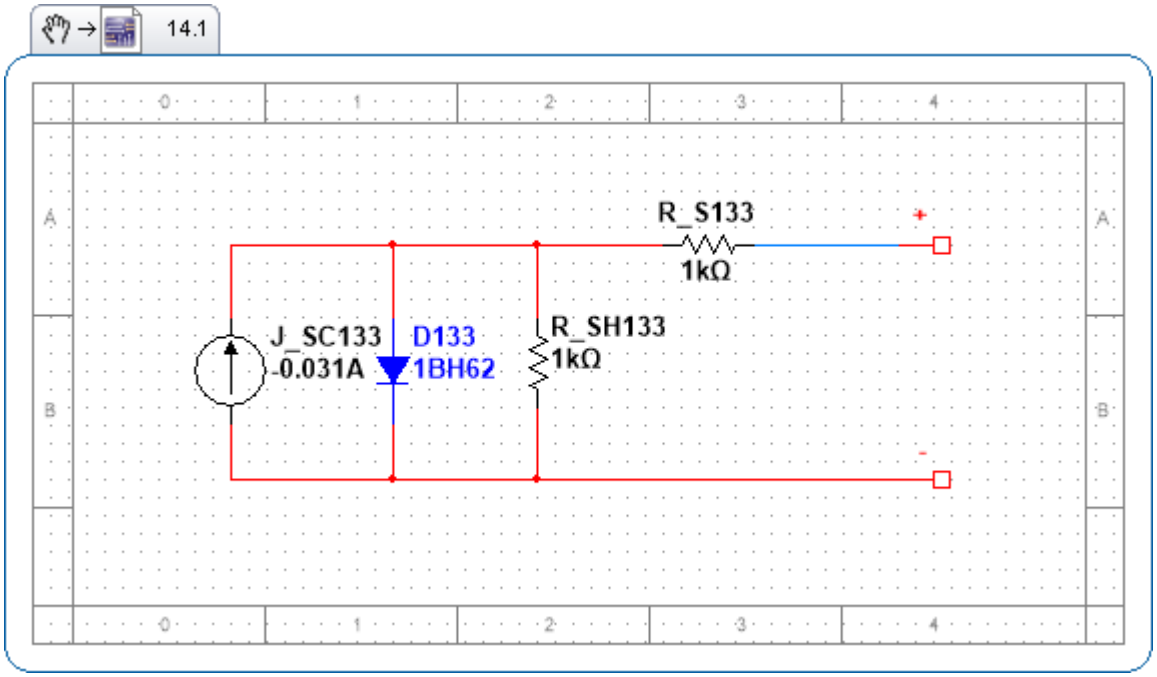

Figure 18 - O.P.V. Base Circuit

3.4.2 Panel

Each wing of the octogon that makes up the Sun-Brella is divided into two sections or *panels*, the reasoning of which is explained in the equivalent CAD chapter of this thesis.

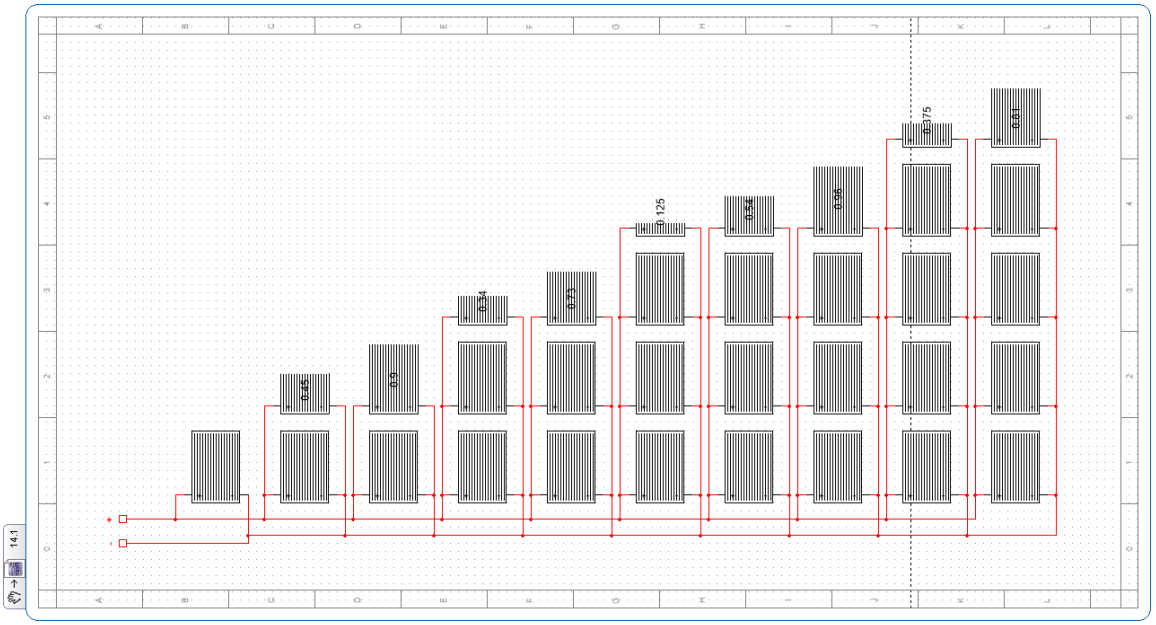

Figure 19 - Panel Circuit

Each panel is a collection of calculations based on the logic previously, and has been done in a parallel circuit to attempt to curb the negative affects of shading that will inevitably occur. For each row within the circuit diagram, the number of base circuits (cells) has been determined by the length of said row divided by the length of the base circuit. This of course left remainders which are accounted for with the fractional cells at the end of most of the rows, with the remainder percentage written on the cell itself as seen in Figure 19. These cells will output an percentage of a base cells current to account for its size descreptancy, and thus allowing for a more accurate model.

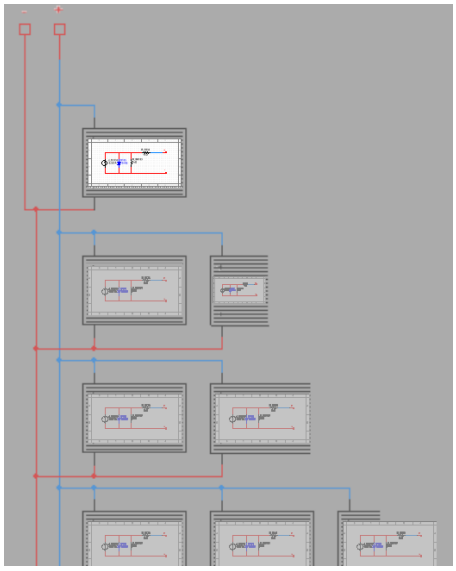

Figure 20 - Panel Base Circuit View

As you can see, each cell is a hierarchical blocking of the base circuit and the length is divided into percentages of the length of the base cell length so as to model the length of the substrate on the CAD model design.

3.4.3 Wing

Continuing in the same vein of attempting to mitigate the inevitable issues that will come up due to the shading of various parts of the Sun-Brella, each panel connection has a bypass diode connected to it. This is meant to allow a path for the circuit to travel that would be unimpeded by a panel that is not producing which, if left un bypassed, would work against the production to a devastating degree.

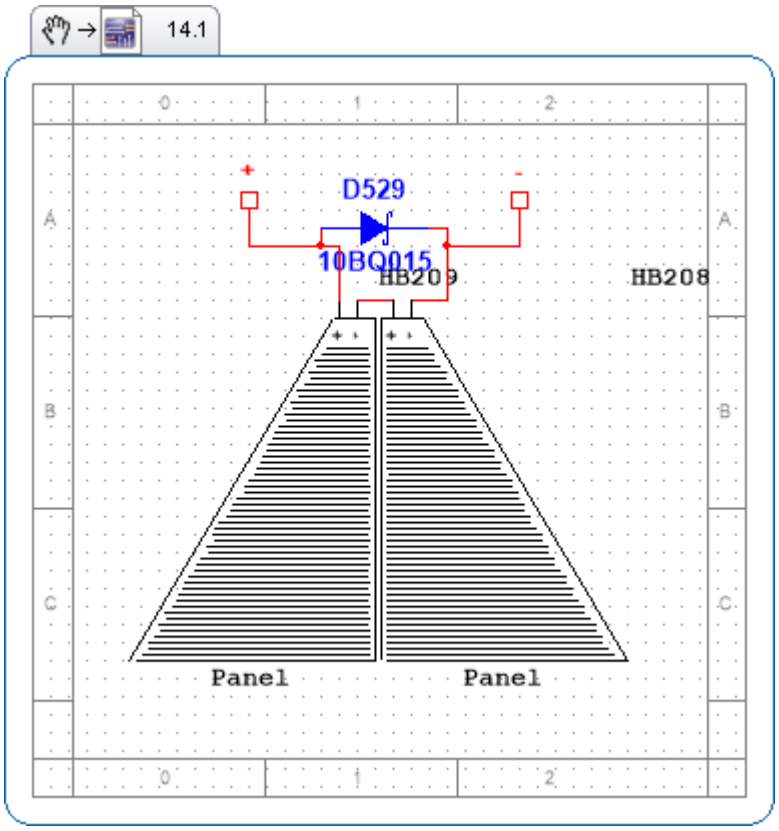

Figure 21 - Wing Circuit

The ideal of a bypass diode between each cell was considered but was left aside until practical tests could be conducted to measure its validity in a parallel circuit system.

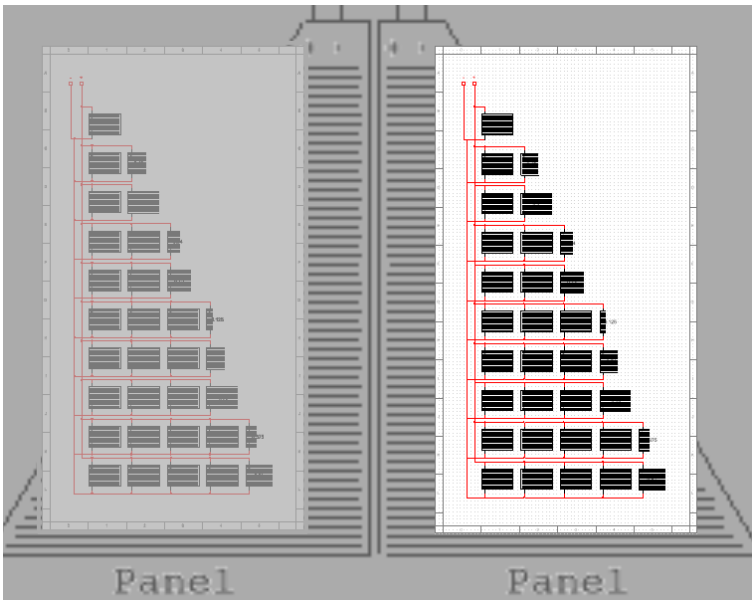

Figure 22 - Wing Panel Circuit View

3.4.4 Master Circuit

This is the entirety of the Sun-Brella circuitry, built as hierarchical blocks from the base cell up to each of the full 8 wings, plus the charge controller at the top running to the battery bank, which then links up to the LED panels under each arm and finally the USB charging circuitry.

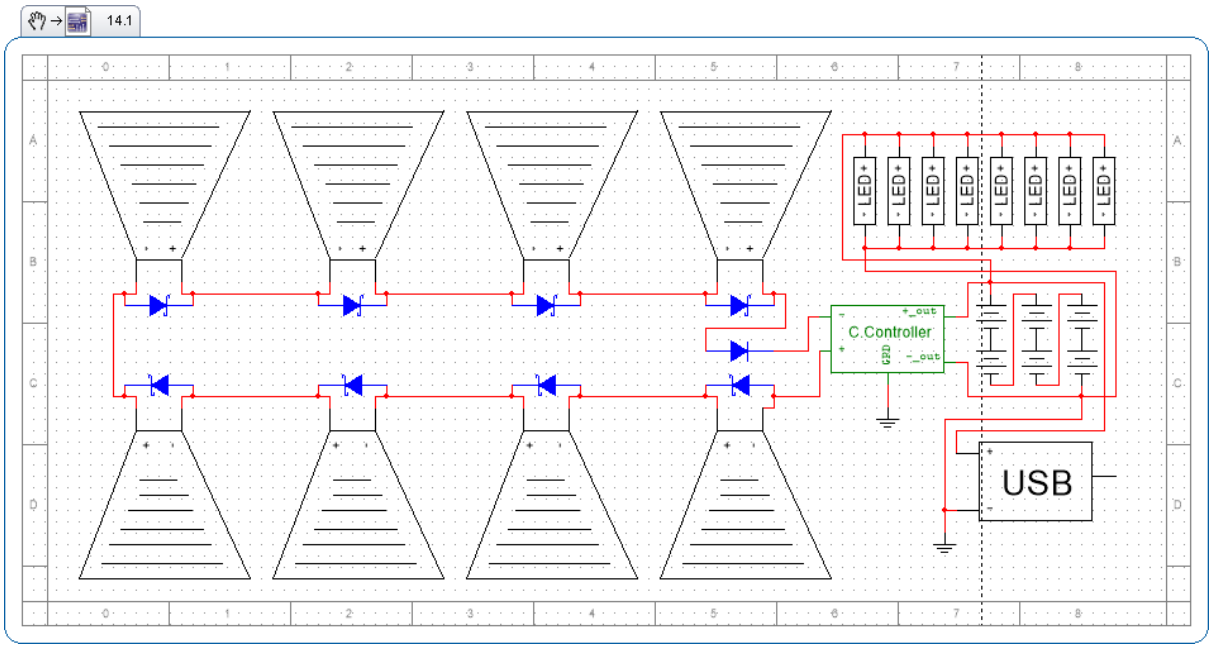

Figure 23 - Master Circuit

To begin, as used before within each wing, each wing itself is connected with a bypass diode to further attempt to mitigate the inevitable effects of shading on the cells. The energy production

begins within the wings and is transmitted into the charge controller. This is necessary due to the unstable properties of each wing. They will not be producing in a consistent manner and to prevent damage to other circuitry within the system the current will pass through the controller before connecting to any other circuitry. Once through the controller it will be transferred to the battery bank. At the moment the batteries are modelled as 6 D cell batteries to allow for simplicity in design. However, this is very likely to be changed in response to the final production values becoming known, and the batteries will be tailored to the production accordingly. Finally, both the LED circuitry and the USB charger are connected to battery bank itself.

3.4.5 LED

The LED strips are models based on the number of LED strips required in the CAD design. This system is set up to only connect to the battery bank for now, however the transistor on the circuit is there to eventually be connected to the charge controller itself so that when light levels dip below a certain level, and thus current/voltage production decreases below a predetermined level, the LEDs will turn on automatically. This will be connected in future improvements to the design, but since many of its variables will be heavily based on the final production value it is only placed there as a reminder of possibilities for now.

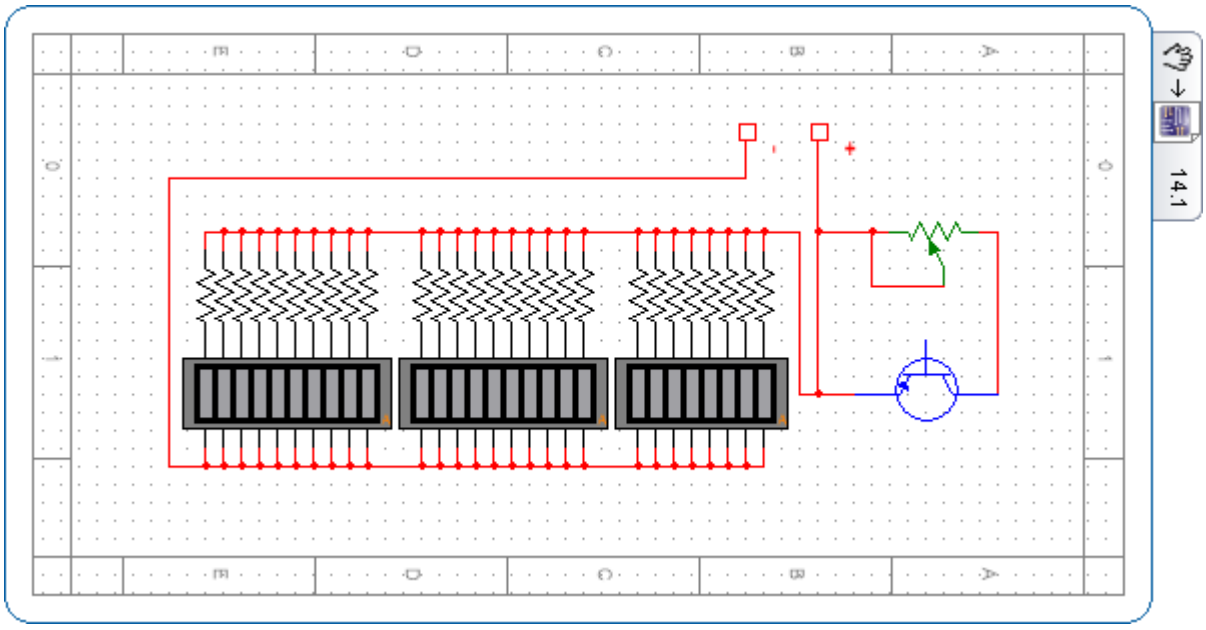

Figure 24 - LED Circuit

3.4.6 USB Charger

Luckily for this design, USB chargers connected to a battery bank does not have values based on the final production value, therefore this is a fully realized circuit. It is a simple circuit, and in the end will most likely be replaced with a pre-made integrated charging circuit PCB, so remains here as an example only.

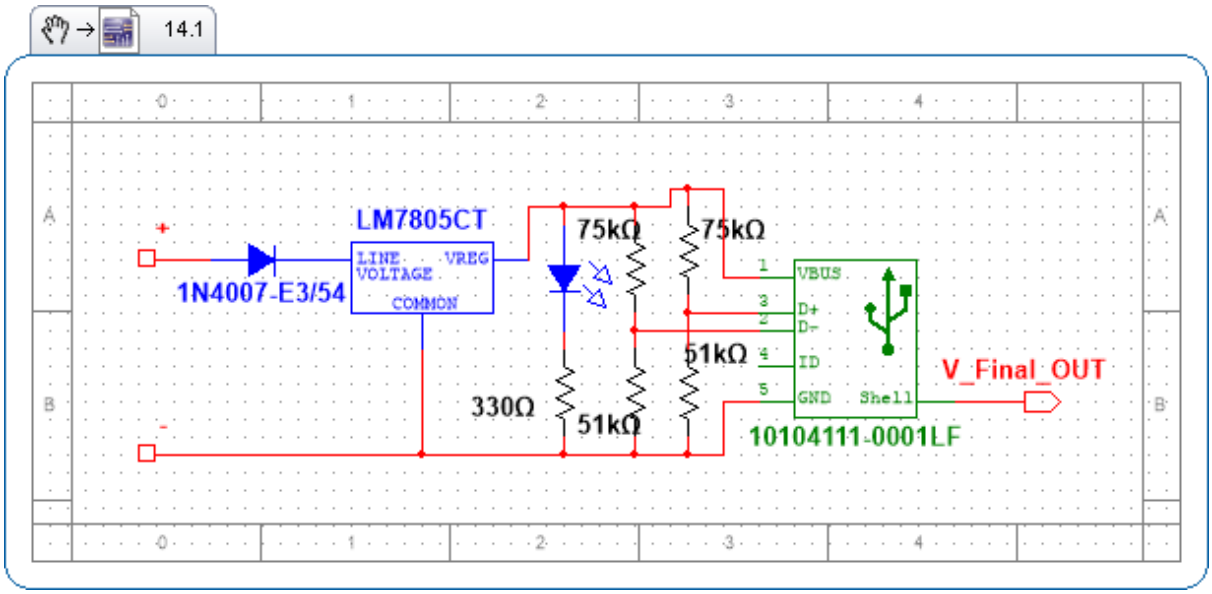

Figure 25 - USB Charger Circuit

4 Analysis

Unfortunately, and disappointingly, the base calculations can only be prepared within the scope of this thesis and no final numbers will be provided. This is due to a lack of availability of the required equipment to measure an accurate IV curve of the base cell itself. This prevents the final calculation since as it is shown in Figure 26,

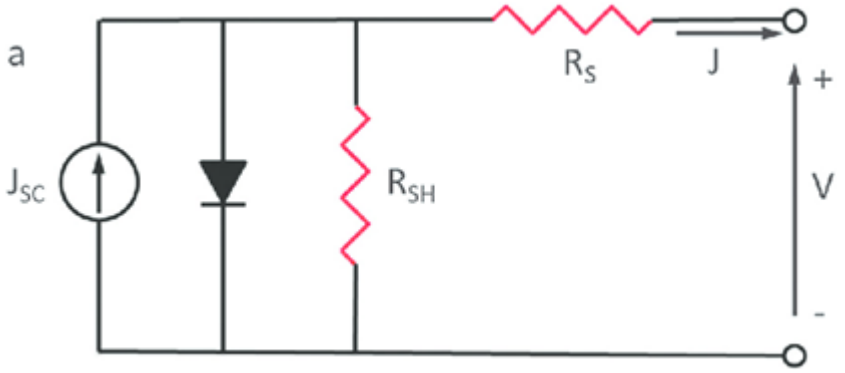

Figure 26 - Base Circuit

(1)

, as the R_s and R_sh, which are the series resistance and shunt resistance respectively, are broadly measured as 1/slope at V_oc and 1/slope at I_sc. Without the ability to accurately obtain slope at those points a working circuit could not be fully modeled. However, everything aside from that has been affectively modeled and only awaits those values; once obtained the final calculations will be available immediately. However, it must be made clear that series and shunt resistance are not fixed values and dependent on irradiance levels. This is made clear by the paper Determination of Internal Series Resistance of PV Devices: Repeatability and Uncertainty (6) where the variability of these values is shown and tested.

Table 1 - Table of R_s and R_sh variations (GT) [6, p. 8]

Meas. Sci. Technol. **27** (2016) 055005 G Trentadue *et al*

Table 4. Variation of electrical performance parameters short circuit current I_{SC}, open circuit voltage V_{OC} and maximum power P_{max} with respect to the reference value taken as that determined with the average series resistance value for two different irradiance translations (50 W m^{-2} and 100 W m^{-2}) and three values of series resistance, 0 Ω and average ±10%.

		50			100		
Device	ΔG (W m^{-2})	ΔI_{SC} (%)	ΔV_{oc} (%)	ΔP_{max} (%)	ΔI_{SC} (%)	ΔV_{oc} (%)	ΔP_{max} (%)
NUF2	$R_S = 0$	−0.0022	−0.568	−0.745	−0.0047	−1.148	−1.485
	R_S +10%	0.0002	0.057	0.082	0.0005	0.115	0.146
	R_S −10%	−0.0002	−0.057	−0.062	−0.0005	−0.115	−0.163
ZZ71	$R_S = 0$	0.0017	−0.469	−0.589	0.0036	−0.965	−1.249
	R_S +10%	−0.0002	0.047	0.076	−0.0004	0.096	0.109
	R_S −10%	0.0002	−0.047	−0.024	0.0004	−0.097	−0.145
TD81	$R_S = 0$	−0.0316	−0.646	−0.815	−0.0662	−1.292	−1.659
	R_S +10%	0.0032	0.065	0.132	0.0066	0.129	0.165
	R_S −10%	−0.0031	−0.065	−0.084	−0.0066	−0.129	−0.149
AY81	$R_S = 0$	−0.0373	−0.744	−0.948	−0.0789	−1.473	−1.850
	R_S +10%	0.0037	0.074	0.126	0.0080	0.147	0.171
	R_S −10%	−0.0037	−0.074	−0.087	−0.0079	−0.147	−0.183
RM81	$R_S = 0$	0.0023	−0.395	−0.496	0.0048	−0.788	−0.946
	R_S +10%	−0.0002	0.039	0.073	−0.0005	0.079	0.126
	R_S −10%	0.0002	−0.039	−0.044	0.0005	−0.079	−0.078
RM82	$R_S = 0$	0.0024	0.423	0.538	0.0046	0.844	1.071
	R_S +10%	−0.0003	−0.042	−0.021	−0.0005	−0.084	−0.105
	R_S −10%	0.0002	0.042	0.079	0.0005	0.084	0.108

As it is shown in Table 1, to get accurate values further testing under controlled circumstances is needed. Unfortunately, until such time as the equipment and tools necessary to provide accurate values for these variables, as stated before, final production results will remain unknown. As for known values, the J_SC of the base circuit has been taken from the data provided by the VTT research team and since its dimensions have been used as the base it will continue to be used as such, at -0.661 mA/cm^2.

As discussed previously, each cell is considered a multiple of the output of this base cell based on its length in respect to the base cell.

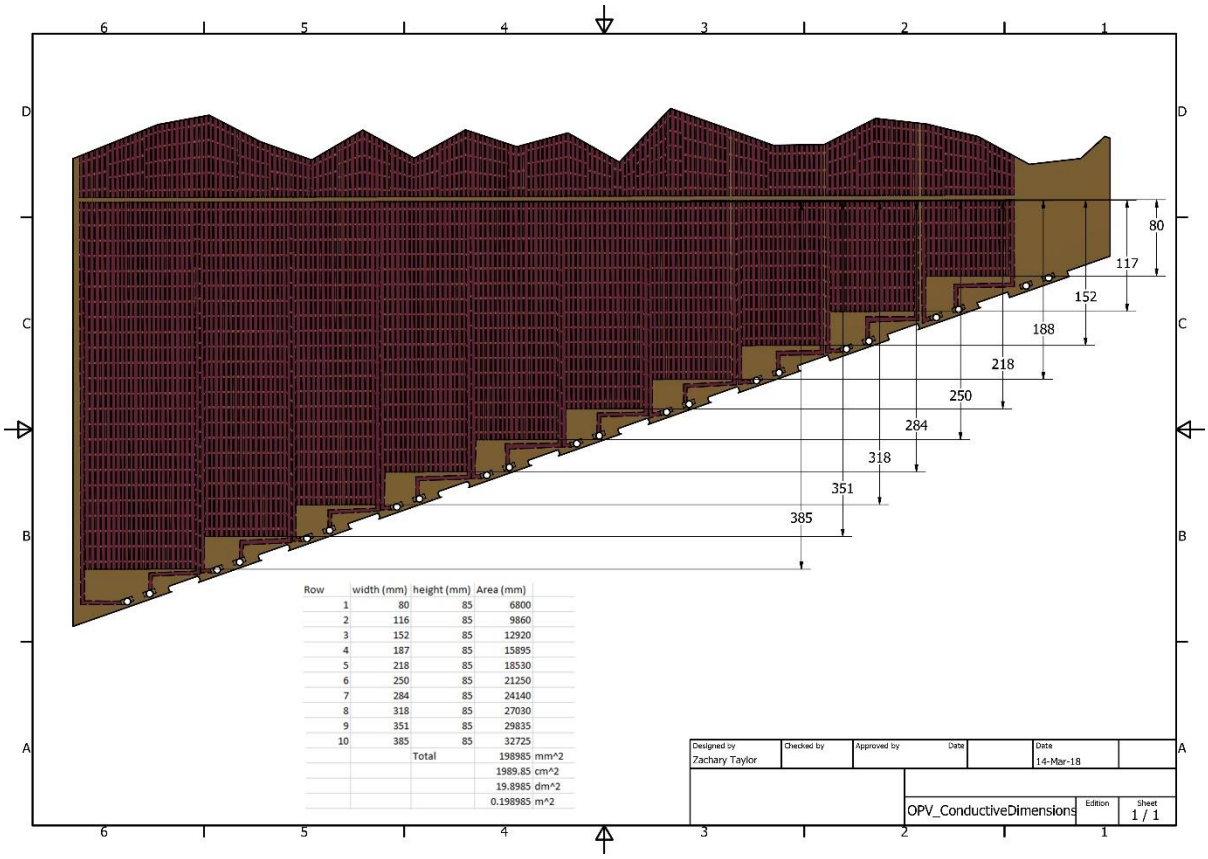

Figure 27 – Base Circuit

This length has been modeled in the circuit diagram and shown/discussed in more detail in the previously mentioned section, but the image is included for easy reference (below)

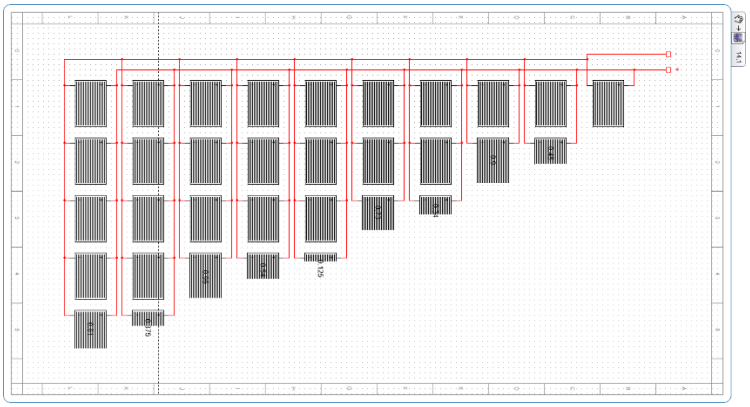

Figure 28 - Copy of Figure 19 (Panel Circuit)

An important note: These calculations are theoretical and under ideal circumstances. Cells linked together will all be limited by those that produce the least current/voltage and there is variation between different individual OPV cells, however this is difficult to account for in

modeling. Once the values are all gathered the final product will be, in practice, ~10-20% less than predicted.

For the final total of surface area of the Sun-Brella's solar cells, it is calculated each panel is approximately 0.19 m^2 with 2 panels per wing, and a total of 8 wings:

$$(0.19\ m^2 * 2) * 8 = \mathbf{3.04\ m^2}$$

This number, as wonderful as it may seem, can be extremely misleading thus one must be careful. With purely theoretical calculations it can be thought to produce significantly more power than reality, as mentioned before. For example, if one took the average irradiance level in the Northern Hemisphere with the conversion efficiency mentioned for O.P.V. material in the Background section with the surface area of the Sun-Brella, one could be misled to believe it could produce upwards of 30 W of power (1000*0.01*30.4=30.4 W), which is undeniably incorrect. Even with considering the 30° tilt of each of the panels; thus, at noon (direct 90°) the power would drop to 26 W (30.4 * cos (30)) at absolute maximum. There are beyond numerous nuances that must be considered as well as a whole host of caveats that will directly affect the actual real-world production value.

The most obvious issue will be the inevitable shading of large sections of the Sun-Brella at any given time. This, in future versions, can be mitigated by the pole tilting apparatus previously mentioned. There is also the issue of the incident angle of the light throughout the day, which as mentioned previously, has been set to 30° to allow for a less severe decrease in power throughout the day without sacrificing the environmental protection of the device.

5 Conclusion

The design of this device has been both extremely rewarding and thought provoking. Initially, the sheer number of individual decisions was considered rather small; however, experience taught otherwise. It was fascinating to see it slowly take shape over the course of so many separate versions of the device, as the final version is technically Sun-Brella 4.0.

The finalization of the upper arm design was the most essential to the entire process as without the many previous versions, it would never have become something that could fulfill as many functions as it currently does.

There is hope that even without a final answer that given the standard conversion efficiency of O.P.V. cells and the area of the device the final production could be within the realms of validity for both powering LED strips and charging a battery bank, however slowly it might do the latter. Worst case there is hope that it could easily power several of the LED strips; this is hard to determine though, since there are so many individual factors associated with LED power usage, but the average seems to be within reasonable limits of the possible production of this device depending on the length of course.

It was very disappointing during the design and circuitry modelling process to come to understand that a final production value was not only difficult to achieve, but well beyond the scope of this thesis. This left a deep and unending desire to continue this project and to see that final value come to fruition, as the answer to the true viability and feasibility of this device is still left up to question. One hopes that the ability to find this answer becomes a possibility in the future. However, in the end, the goal of this thesis has always been to attempt to create a viable working model of a Sun-Brella and in that it was a success.

There are many aspects that could have been both done better and differently, such as doing significantly more extensive research before starting the build process. This would have been wonderful as more energy could have been put toward attempting to secure the necessary equipment so that all the variables could be accounted for. However, this would have delayed or prevented the design of the device entirely; thus, it may have been for the best.

As mentioned throughout the thesis, there is a laundry list of improvements that could be done on both the wiring and the design of the Sun-Brella itself to make it more efficient and useful. There are so many unknowns that this thesis is nothing more than a starting point for the possible creation of such a device. There is still the unknown of the final power output, there is no testing done of the optimum angle for power output throughout a day, no calculation done on optimum battery bank, no determination of optimum charge controller configuration, configuration changes due to printing technique specifications, and the list continues.

It is a sincere hope and goal of the author to continue the work being done on this device, which has the potential to be a part of the renewable energy revolution currently happening today, and to see its eventual fruition in one form or another.

References

1 Wikipedia contributors. Ching W. Tang [Internet]. Wikipedia, The Free Encyclopedia; 2018 Jan 31, 19:04 UTC [cited 2018 March 10]. Available from: https://en.wikipedia.org/w/index.php?title=Ching_W._Tang&oldid=823351241.

2 Spanggaard, H., Krebs, F. *A brief history of the development of organic and polymeric photovoltaics*. Science Direct, [document on the Internet]. 2004 [cited 2018 March 13]; 83 part 2, 125-146. Available from: http://www.sciencedirect.com/science/article/pii/S0927024804000923

3 Hanania, J., Stenhouse, K., Yyelland, B., Donev, J. Photovoltaic Effect. Energy Education [document on the Internet] 2018 [cited 2018 March 19] Available from: http://energyeducation.ca/encyclopedia/Photovoltaic_effect

4 Apilo, P. *Roll-to-roll printing of organic photovoltaic cells and modules*. Doctor of Science in Technology. [thesis]. Oulu, Finland: University of Oulu

5 Mazzio, K., Luscombe, C. *Corrections: The future of organic photovoltaics.* Research Gate, [document on the Internet]. 2014 [cited 2018 March 19] Available from: https://www.researchgate.net/publication/265412308_Correction_The_future_of_organic_photovoltaics

6 Kippelen, B., Choi, S., Potscavage, W.J. *Modeling large-area solar cells*. Center for Organic Photonics and Electronics; School of Electrical and Computer Engineering: Georgia Institute of Technology., [document on the Internet]. 2018 [cited 2018 March 19] Available from: https://ieeexplore.ieee.org/document/5595664

7 Trentadue, G. et al. *Determination of internal series resistance of PV devices: repeatability and uncertainty*. IOP Publishing Meas.Sci.Technol, [document on the Internet]. 2016 [cited 2018 March 19] 27, 055005. Available from: http://iopscience.iop.org/article/10.1088/0957-0233/27/5/055005/pdf

8 Laube, P. *Semiconductor Technology - Fundamentals*. Halbleitor, [Online]. 1.1 Conductors-Insulators- Semiconductors [document on the Internet] 2017 [cited 2018 March 19] p. 6. Available at: https://www.halbleiter.org/en/fundamentals/conductors-insulators-semiconductors/

Appendix 1. CAD Drawings – Sun-Brella Assembly and Parts List

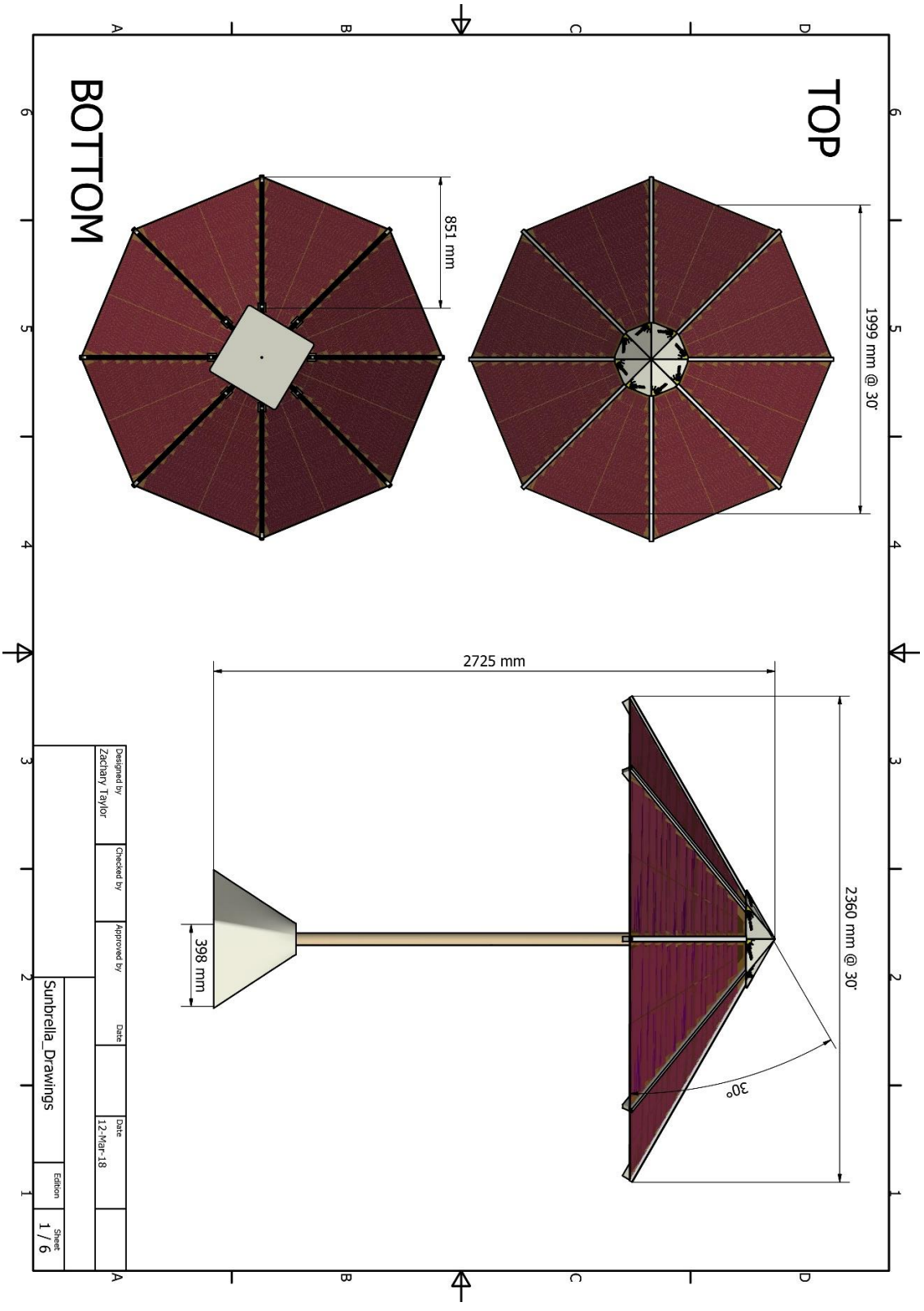

Drawing 1 - Sunbrella Top/Bottom

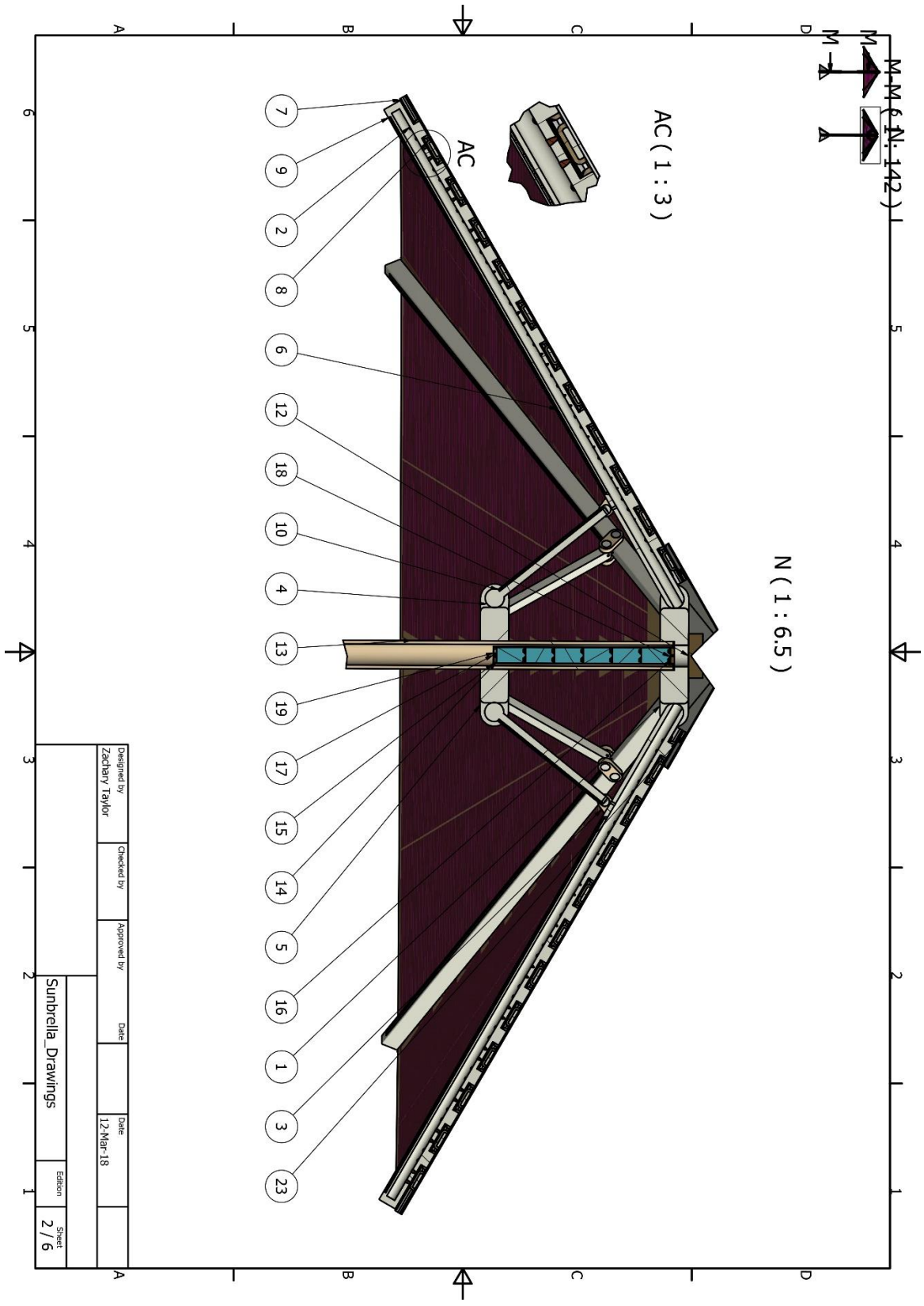

Drawing 2 - Sunbrella Top Cut

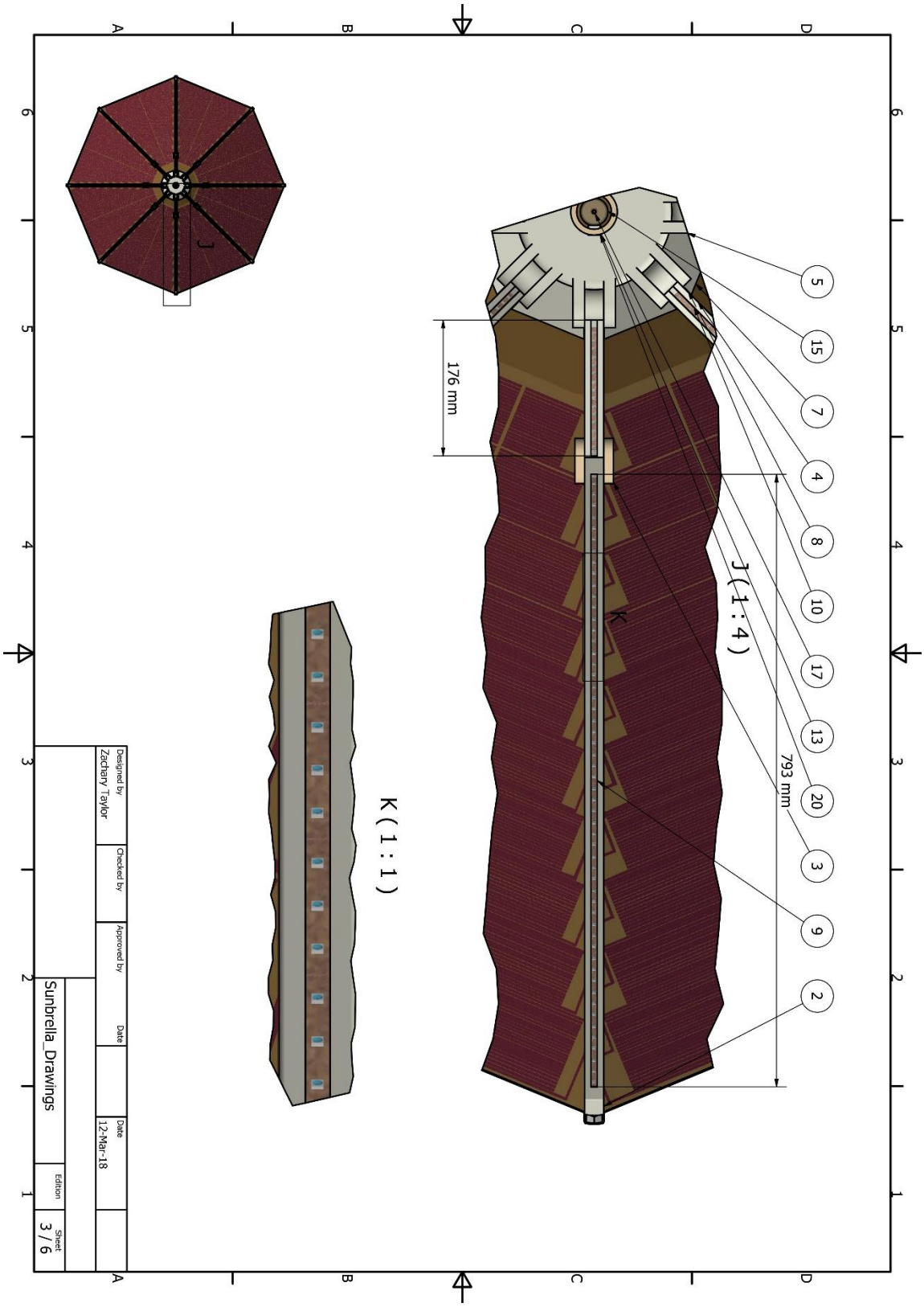

Drawing 3 - Sunbrella Under Top Arm

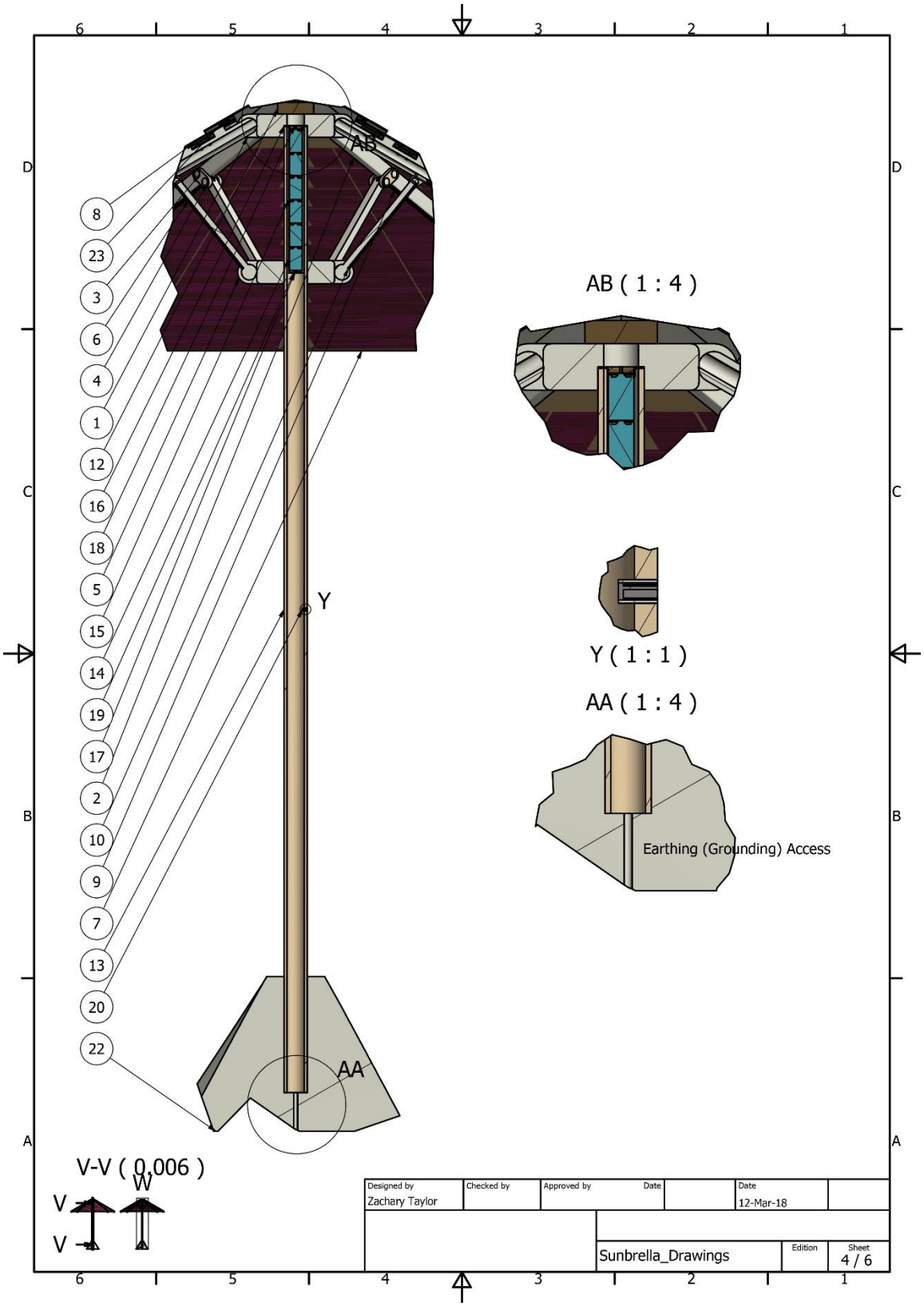

Drawing 4 - Long Pole Cut

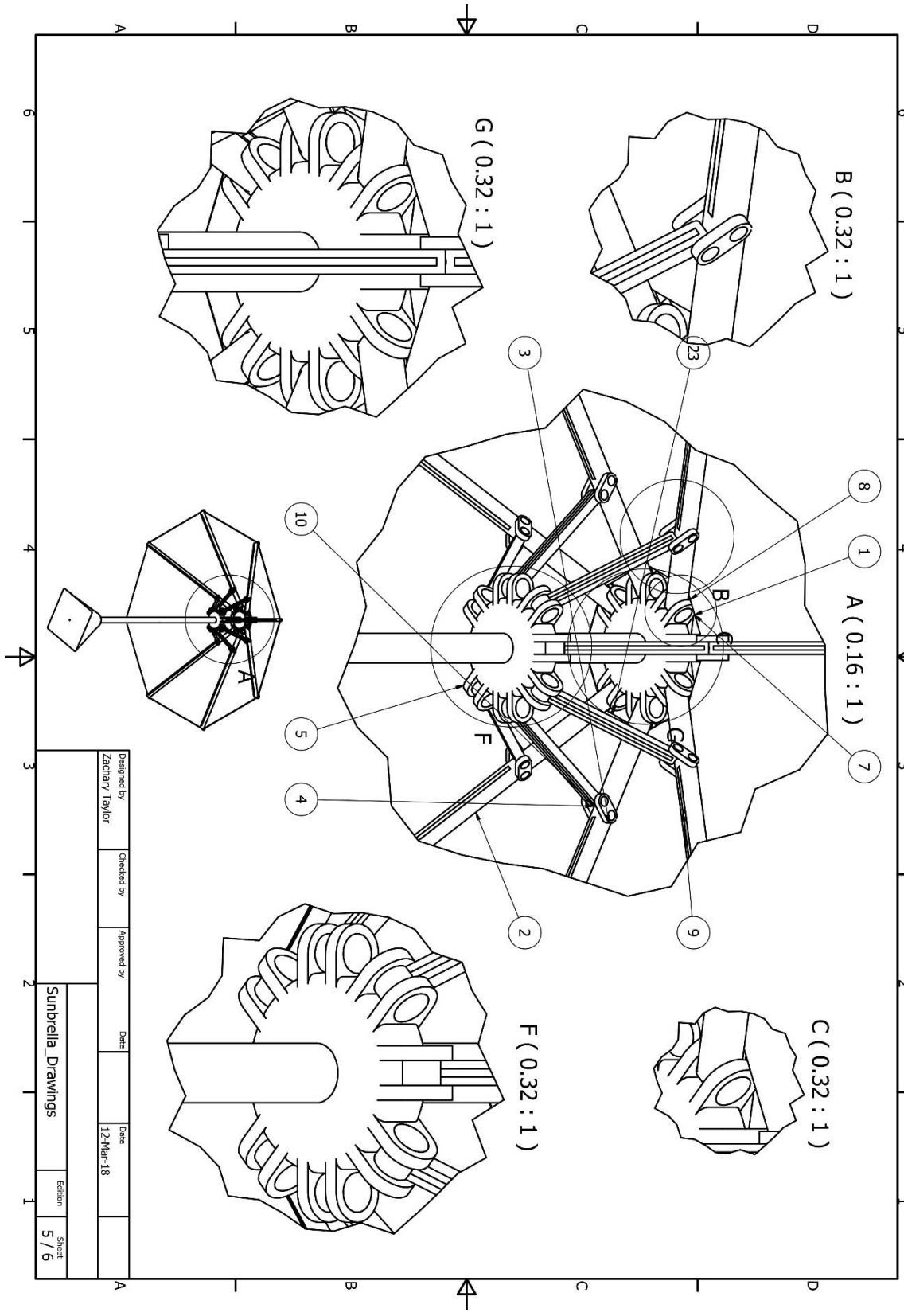

Drawing 5 - Sunbrella Support Structure

PARTS LIST			
ITEM	QTY	PART NUMBER	DESCRIPTION
1	1	Octogon_top	Upper disc containing electronics and cover
2	8	Arm_top	Housing for terminals and internal wiring, and physical support (LED inbedded)
3	16	connector	connects upper and lower arms
4	8	Arm_bottom	connects upper arm to lower octagon (LED inbedded)
5	1	Octogon_bottom	Physical support for Umbrella structure to Pole, movable (no electronic parts)
6	184	LED Strip	Self-explanatory, inbedded in each of the 8 upper/lower arm pairs
7	8	OPV	Self-explanatory, Electricity production begins here
8	8	Arm_sheath	Environmental shielding for +/- Terminals on each upper arm, plus connector for Cover
9	8	LED_shield_top	Environmental covering for upper LED strip
10	8	LED_shield_bottom	Environmental covering for lower LED strip
11	8	Sunbrella.Harness	Electrical Wiring for all OPV and Charge Controller to Battery terminal
12	1	ChargeController	Self-explanatory, controls electricity quality to battery terminal
13	1	Pole	Main physical support structure
14	6	D Cell	Battery (open for adaptation based on power output)
15	1	BatteryHousing	Container for all Battery storage
16	1	BatteryCap.iam	Physical connection to Pole, provides terminal for battery storage
17	1	Batterybottom_pin	conductive terminal in battery housing
18	1	BatteryCap_pin	conductive terminal in battery housing
19	1	Spring	Physical pressure to ensure conductive path
20	1	USB Port final	USB port for devices to interact with power station
21	1	Sunbrella.Harness2	Electricity wiring from Battery Terminal to USB port and Earth
22	1	Stand	Physical support structure for Pole
23	1	Cover	Environmental protection for all electronics (charge controller, etc)

Designed by	Checked by	Approved by	Date		Date	
Zachary Taylor					12-Mar-18	

Sunbrella_Drawings	Edition	Sheet 6 / 6	

Drawing 6 - Sunbrella Parts List

Appendix 2. CAD Drawings – Individual Parts

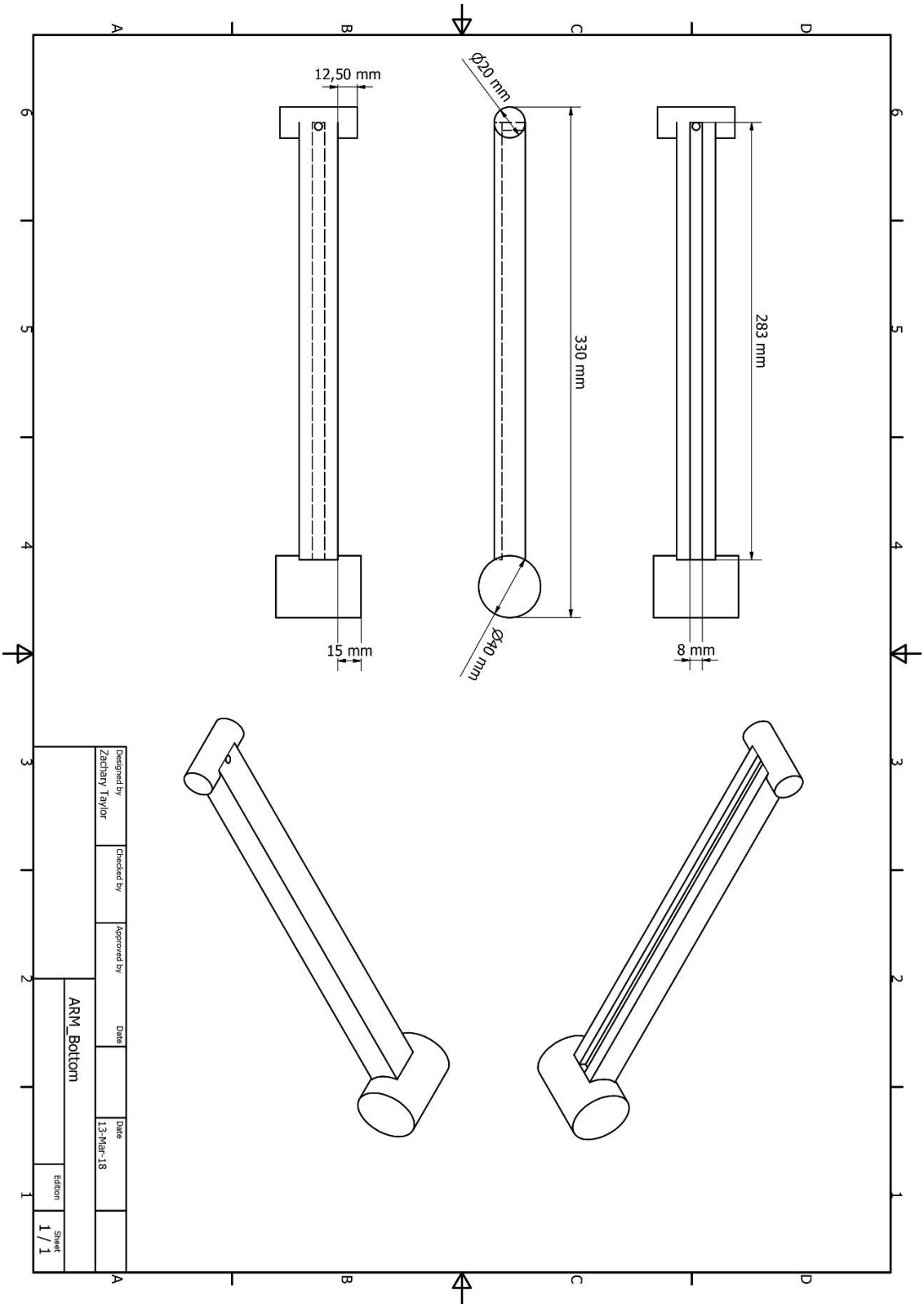

Drawing 7 - Bottom Arm

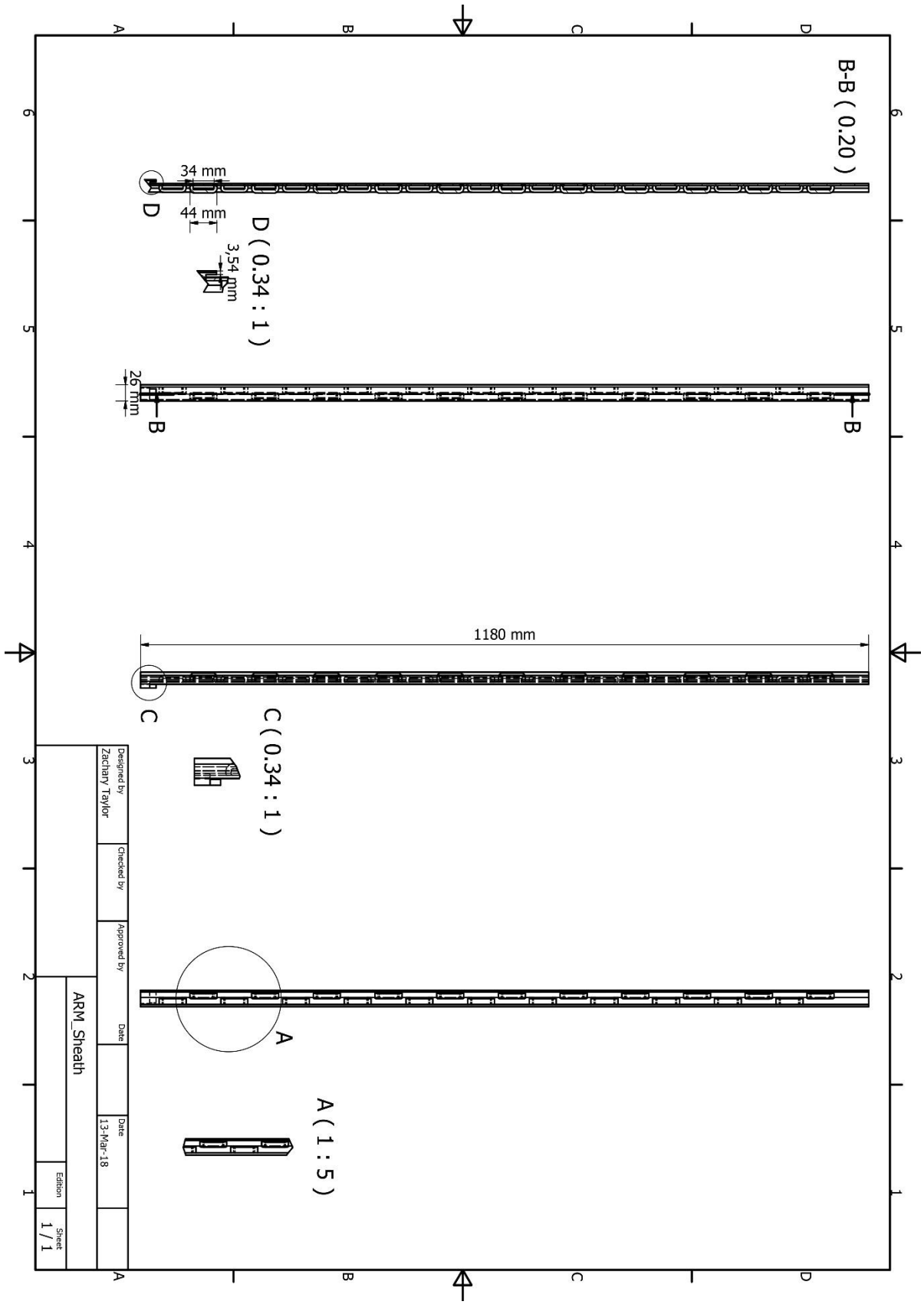

Drawing 8 - Arm Sheath

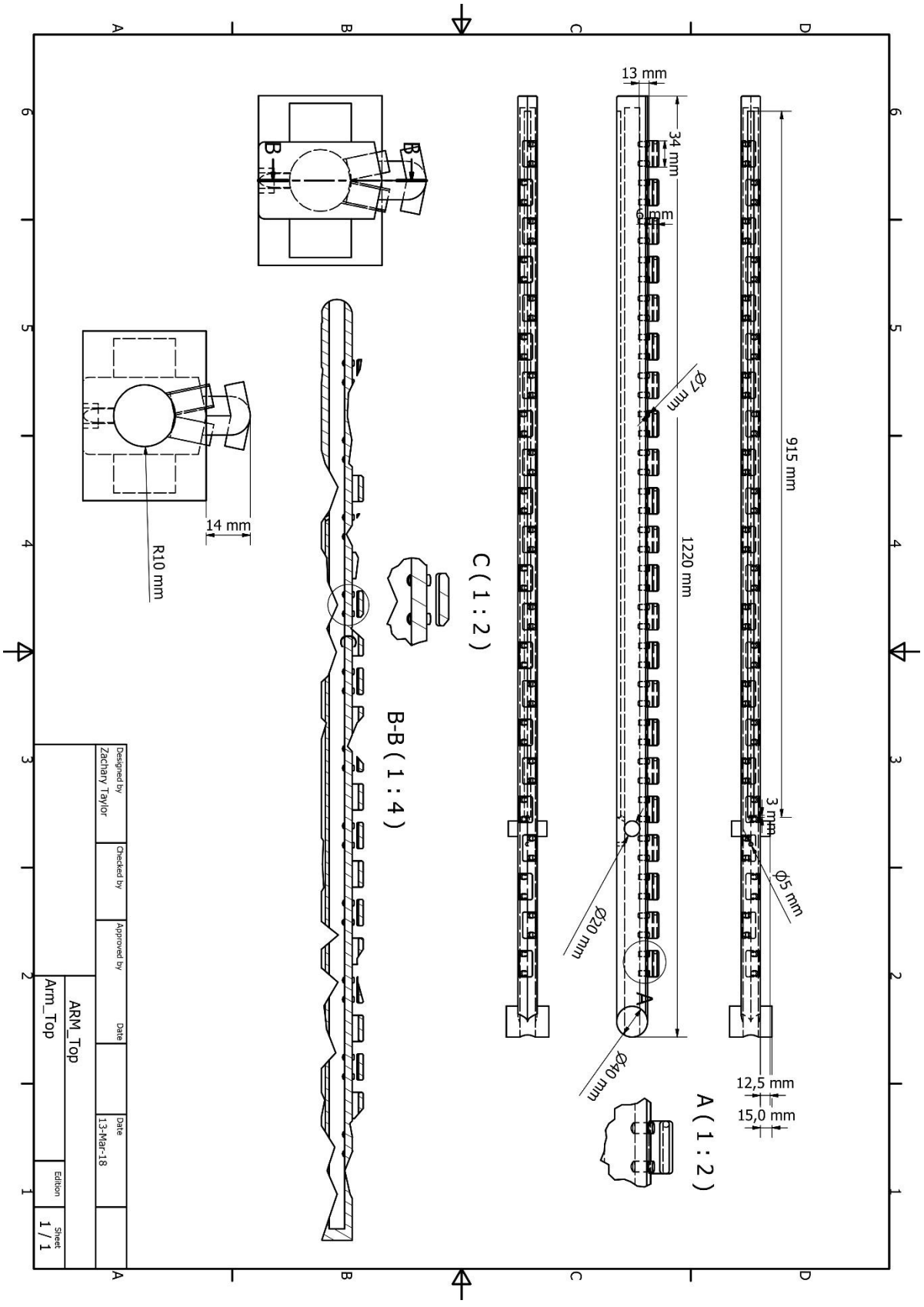

Drawing 9 - Top Arm

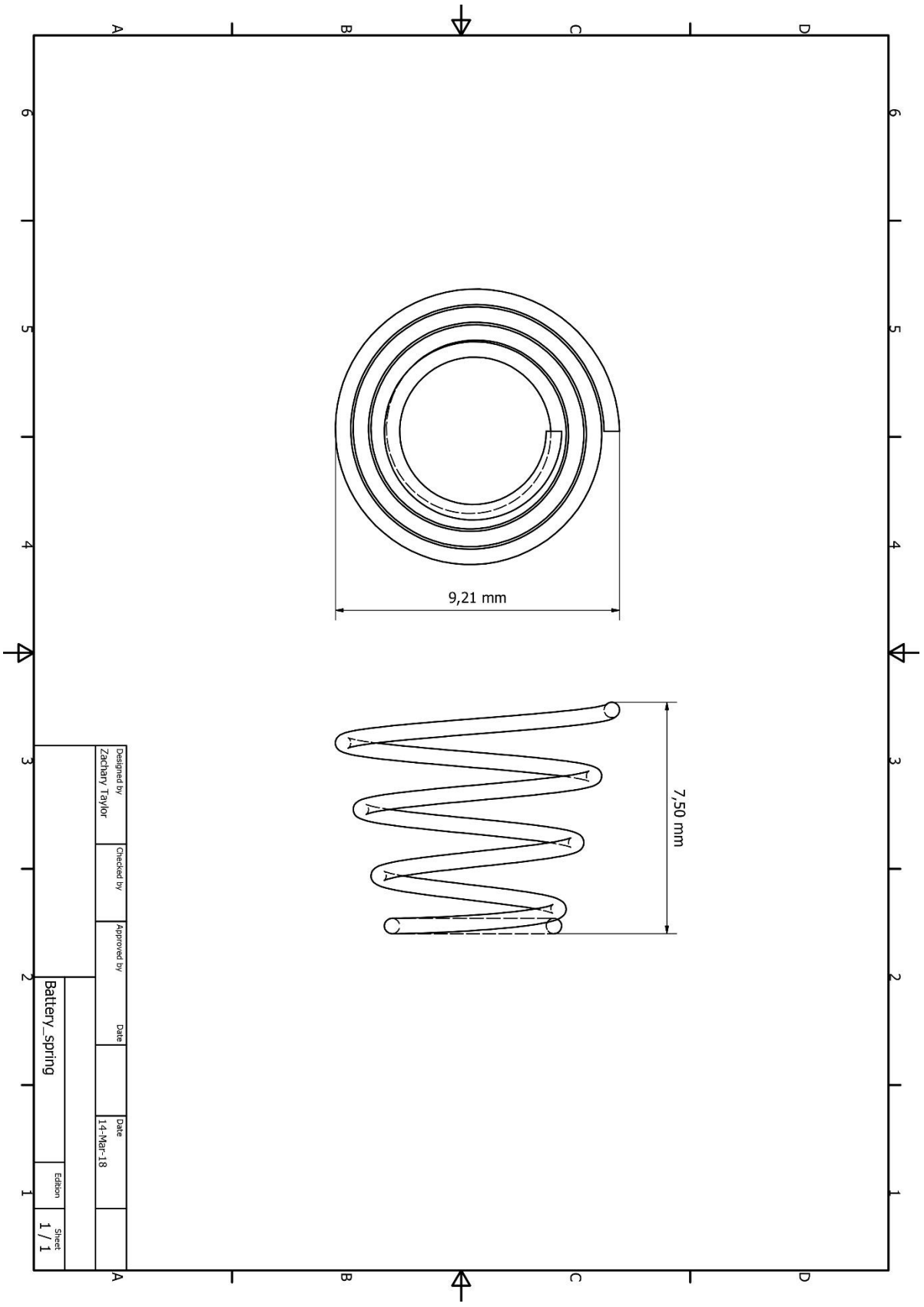

Drawing 10 - Battery Spring

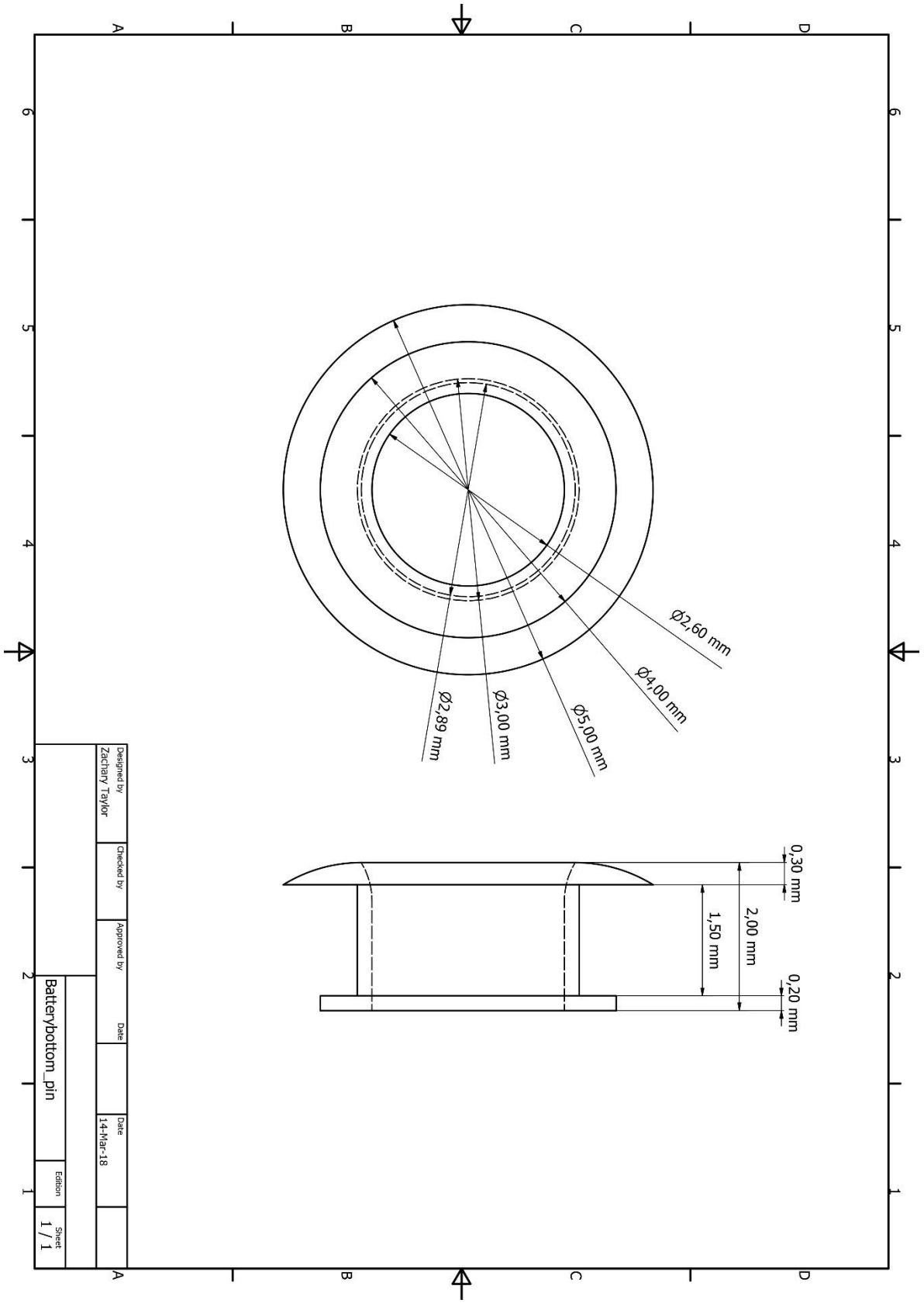

Drawing 11 - Battery Bottom Pin

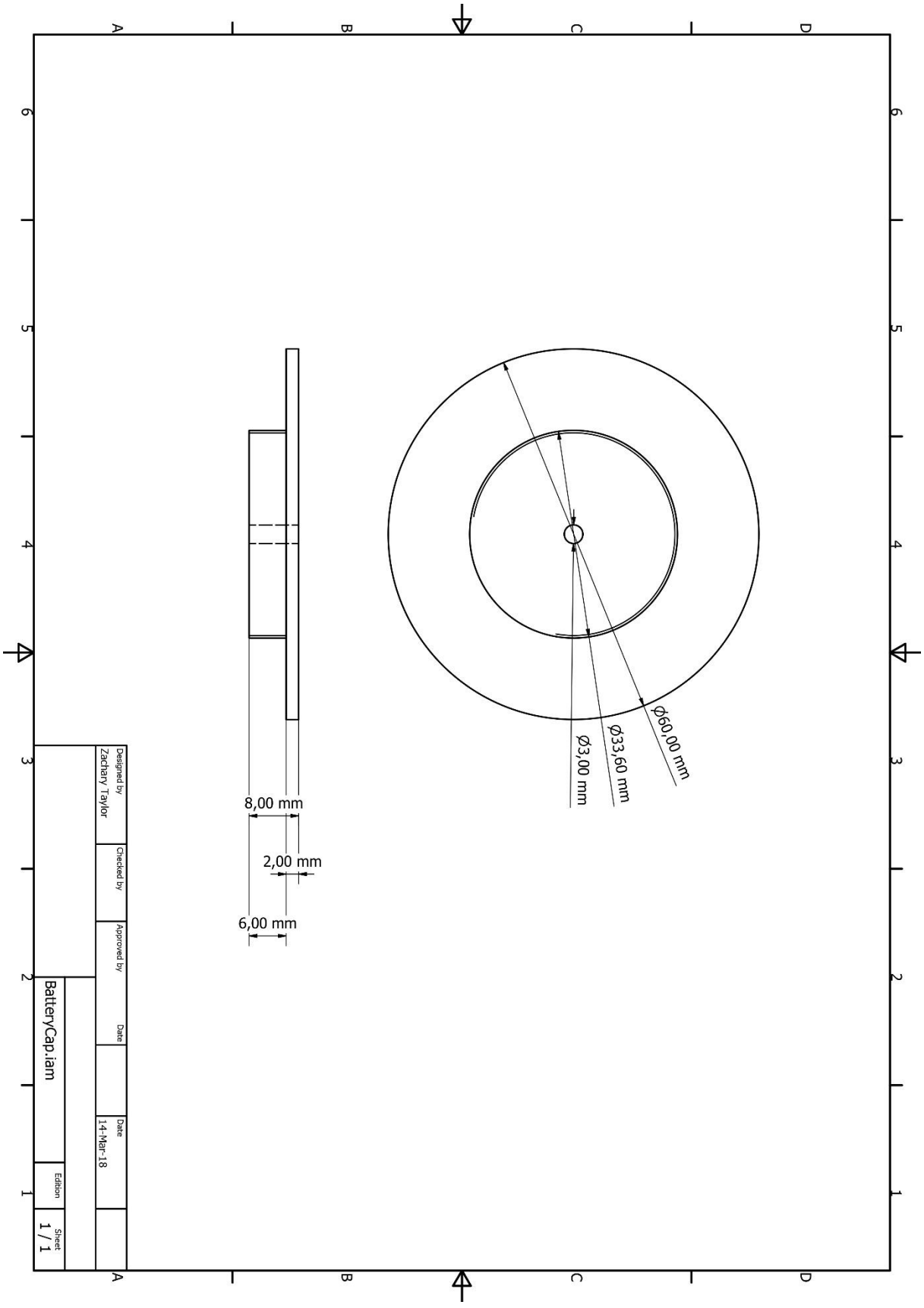

Drawing 12 - Battery Cap

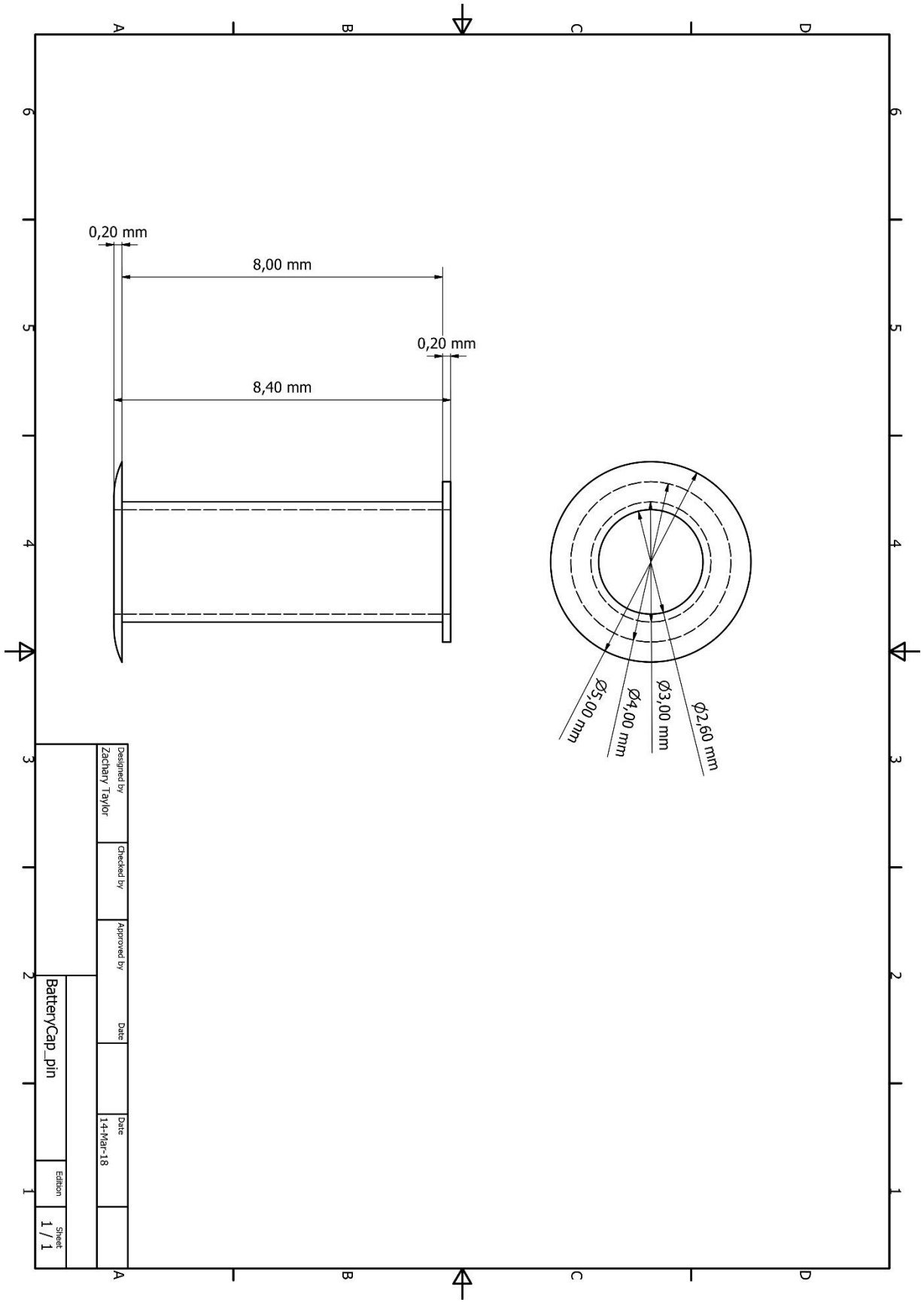

Drawing 13 - Battery Cap Pin

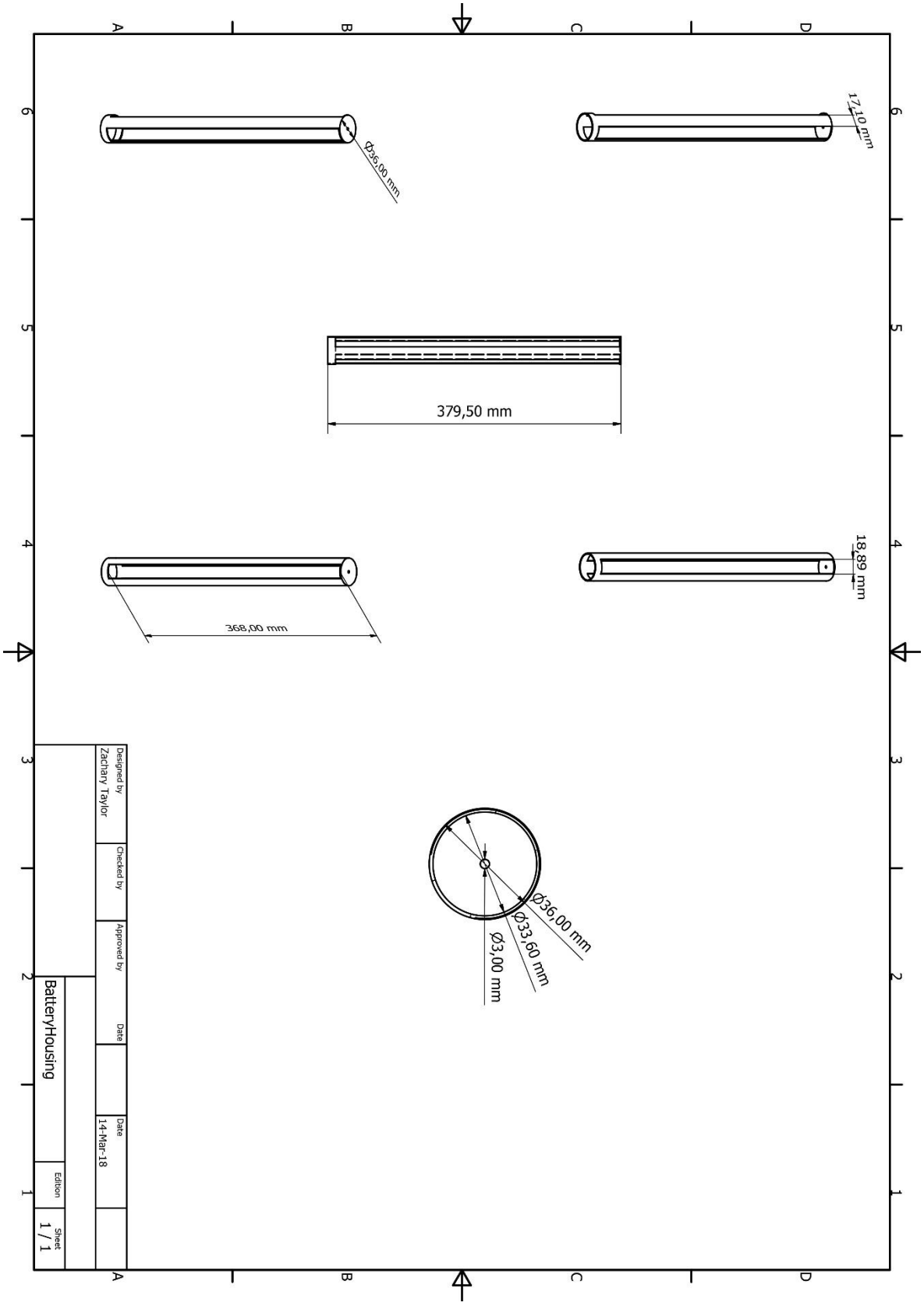

Drawing 14 - Battery Housing

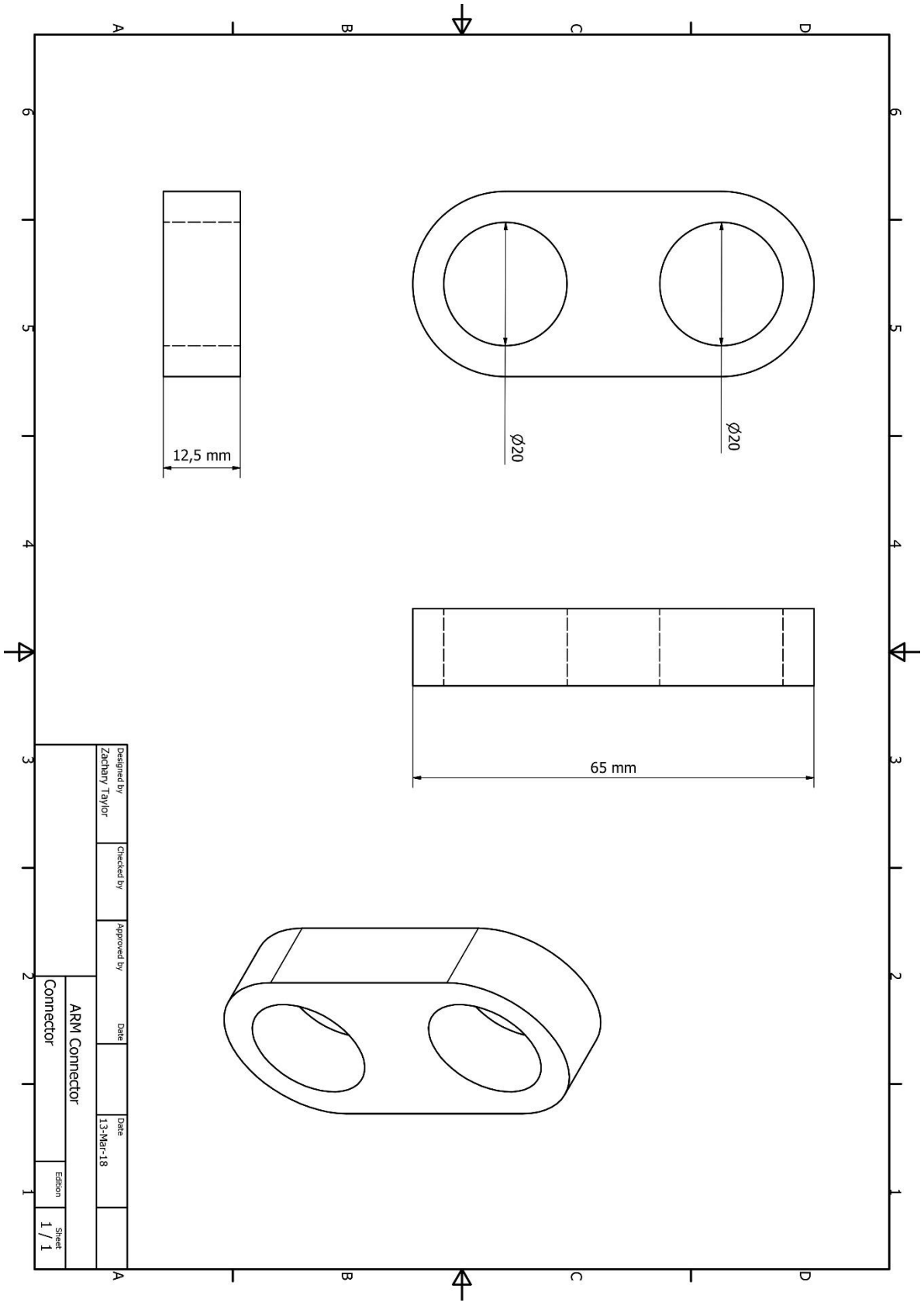

Drawing 15 - Arm Connector

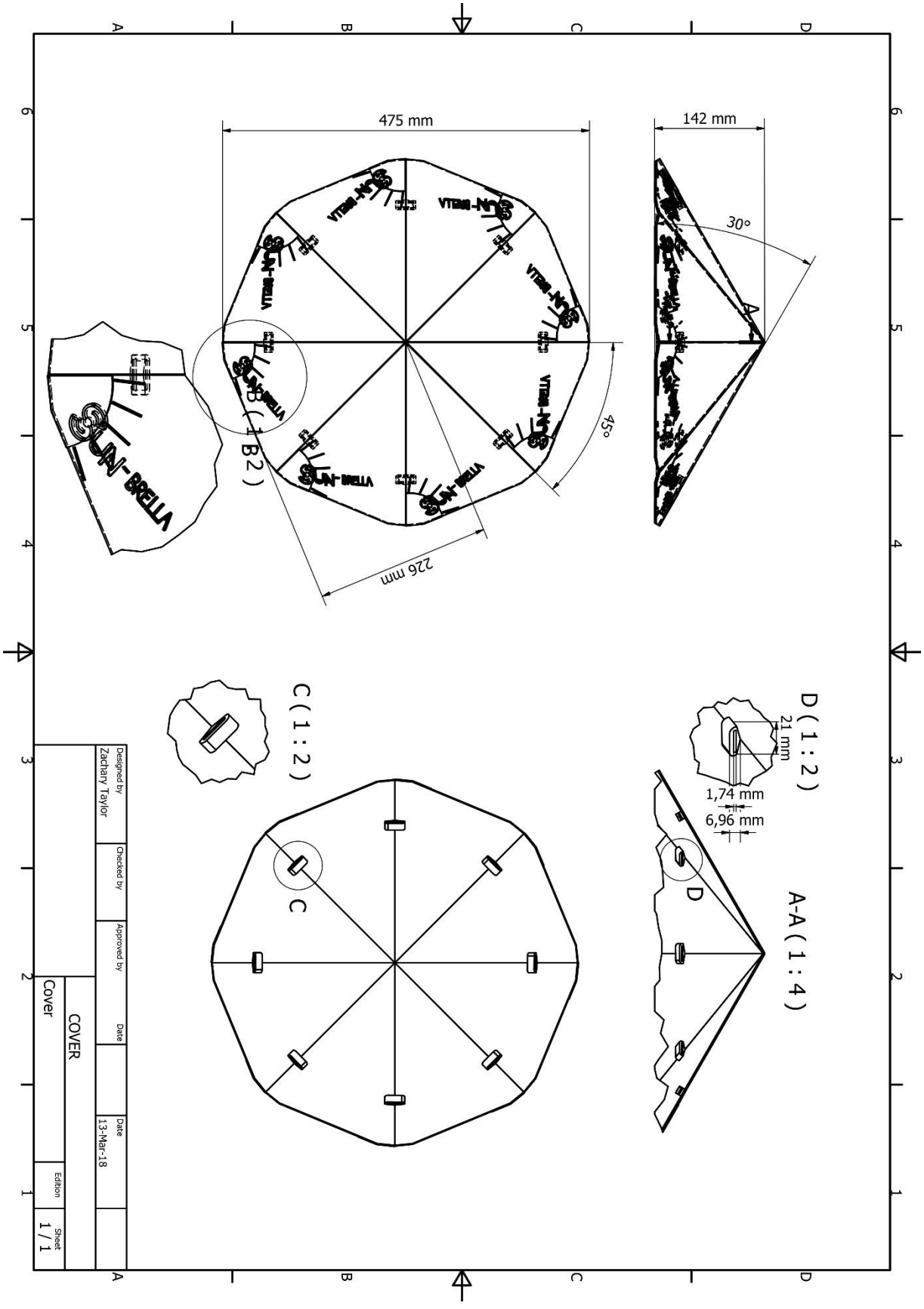

Drawing 16 - Cover

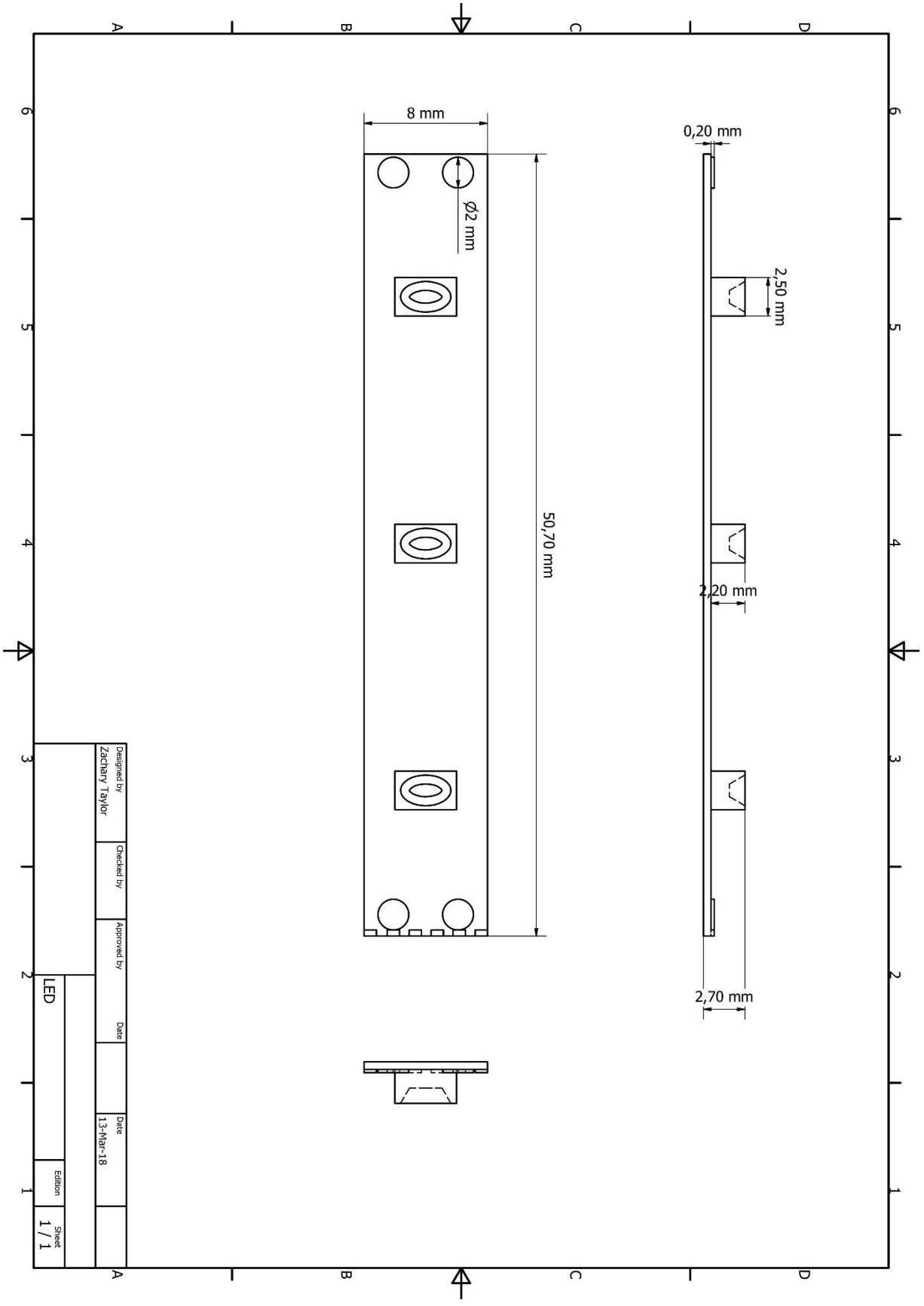

Drawing 17 - LED

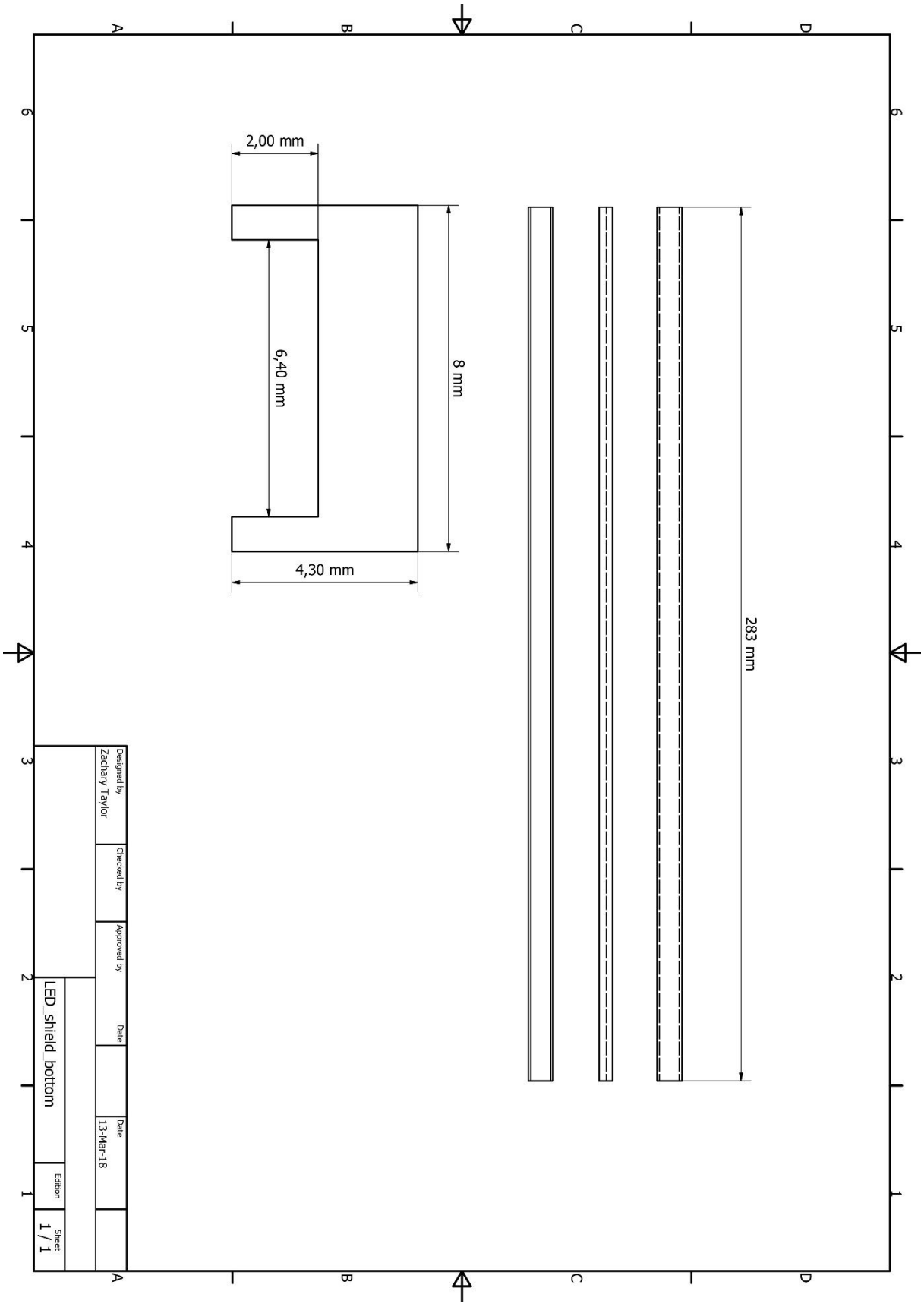

Drawing 18 - LED Bottom Shield

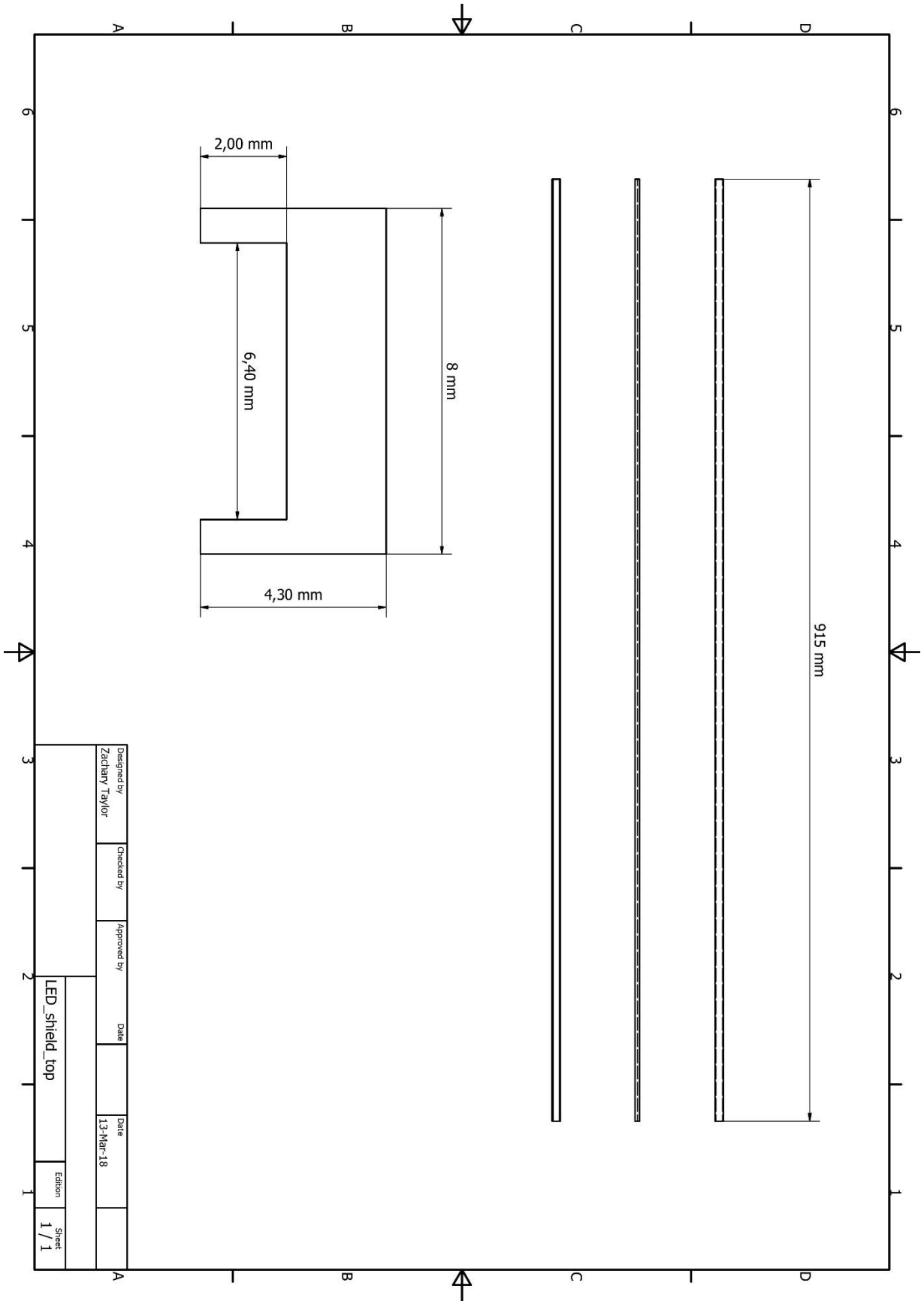

Drawing 19 - LED Top Shield

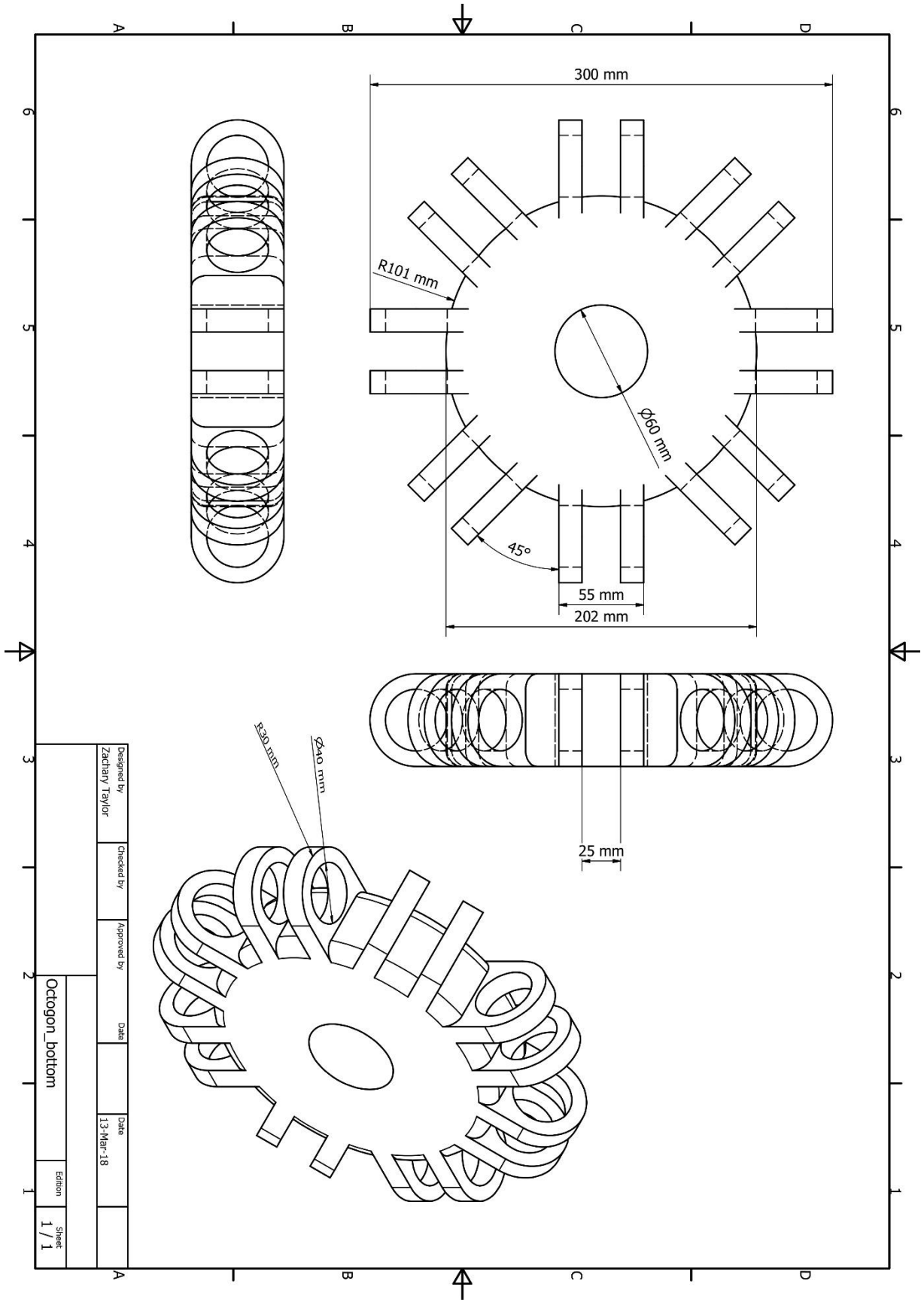

Drawing 20 - Bottom Octagon

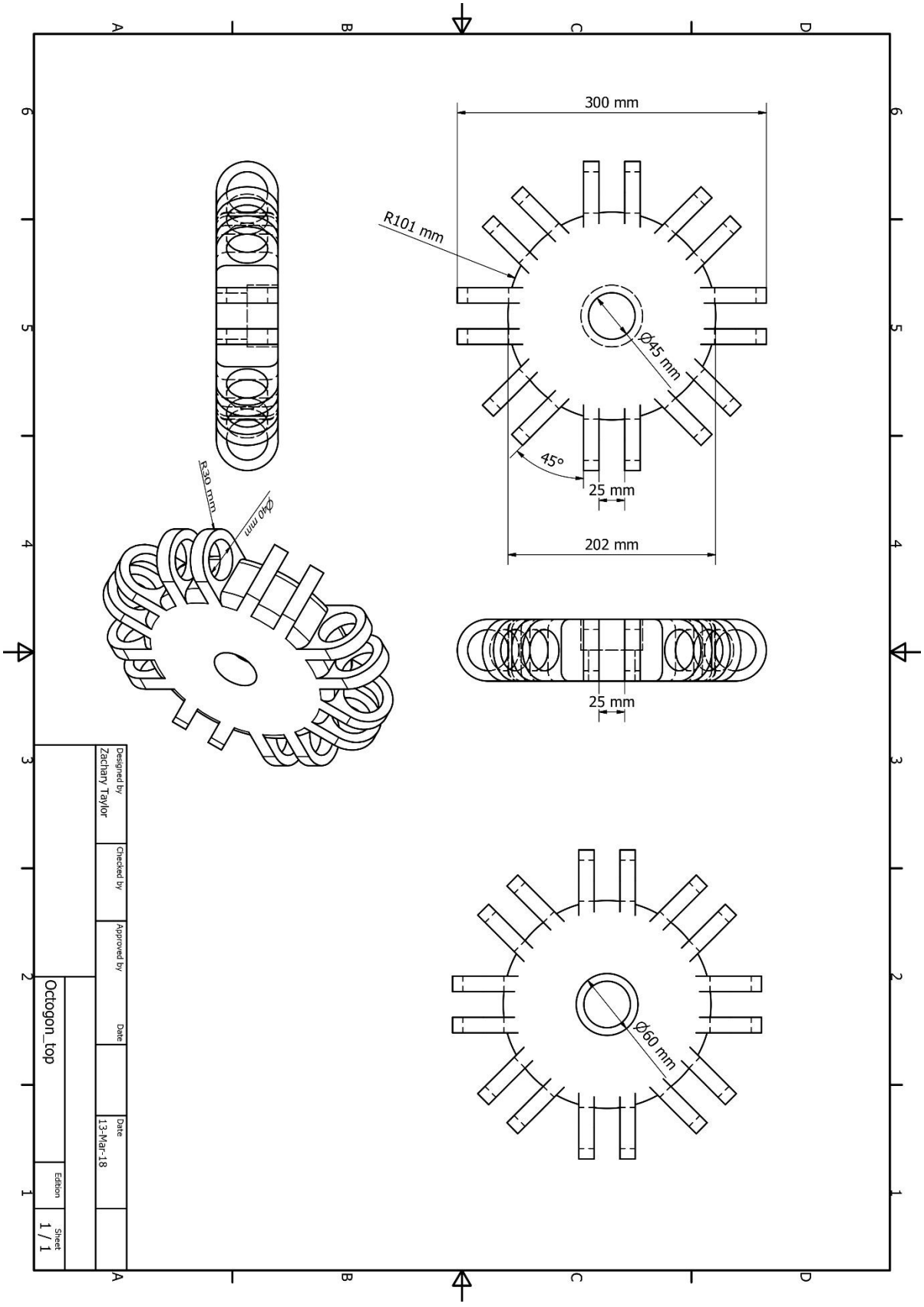

Drawing 21 - Top Octagon

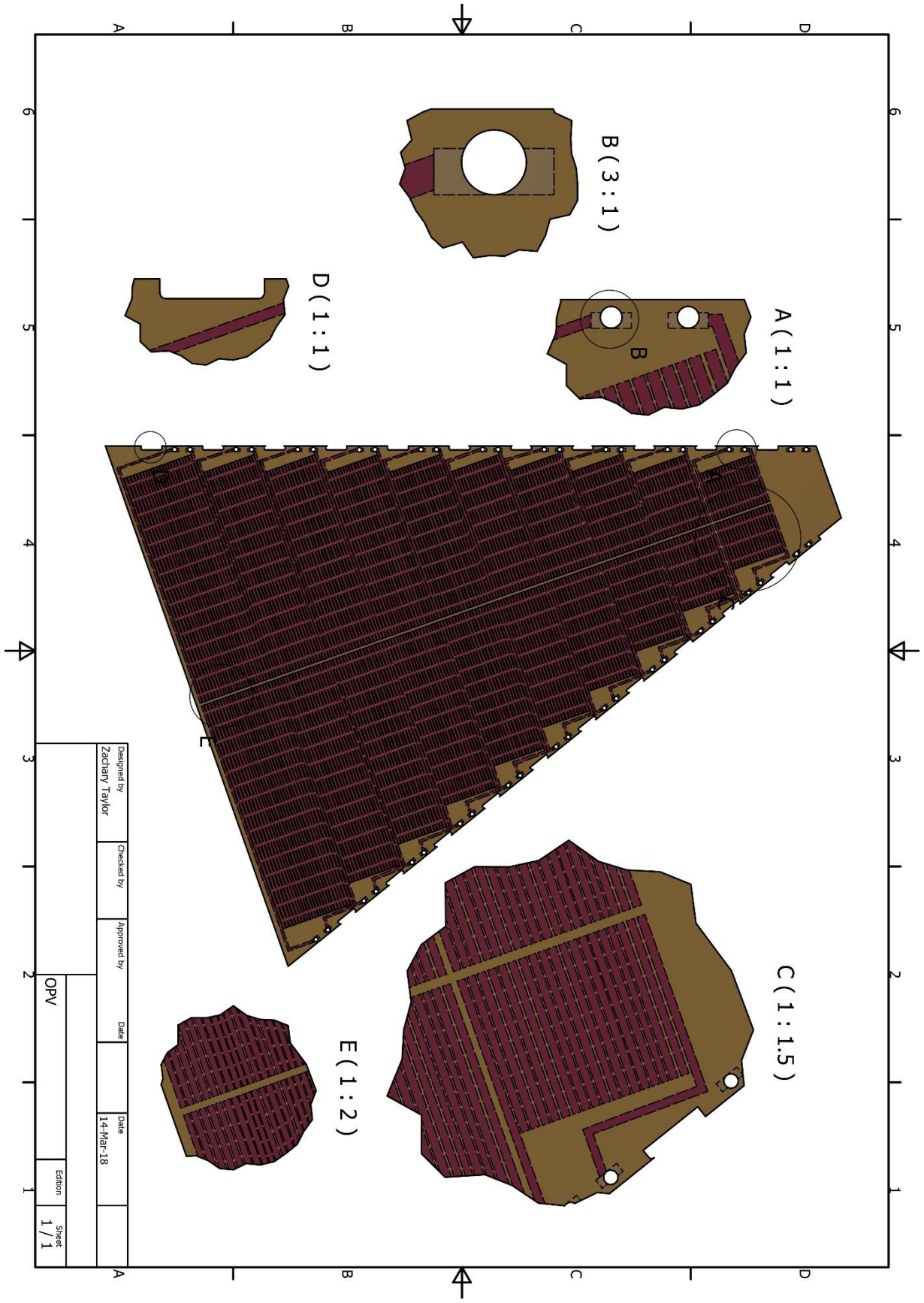

Drawing 22 - OPV Wing

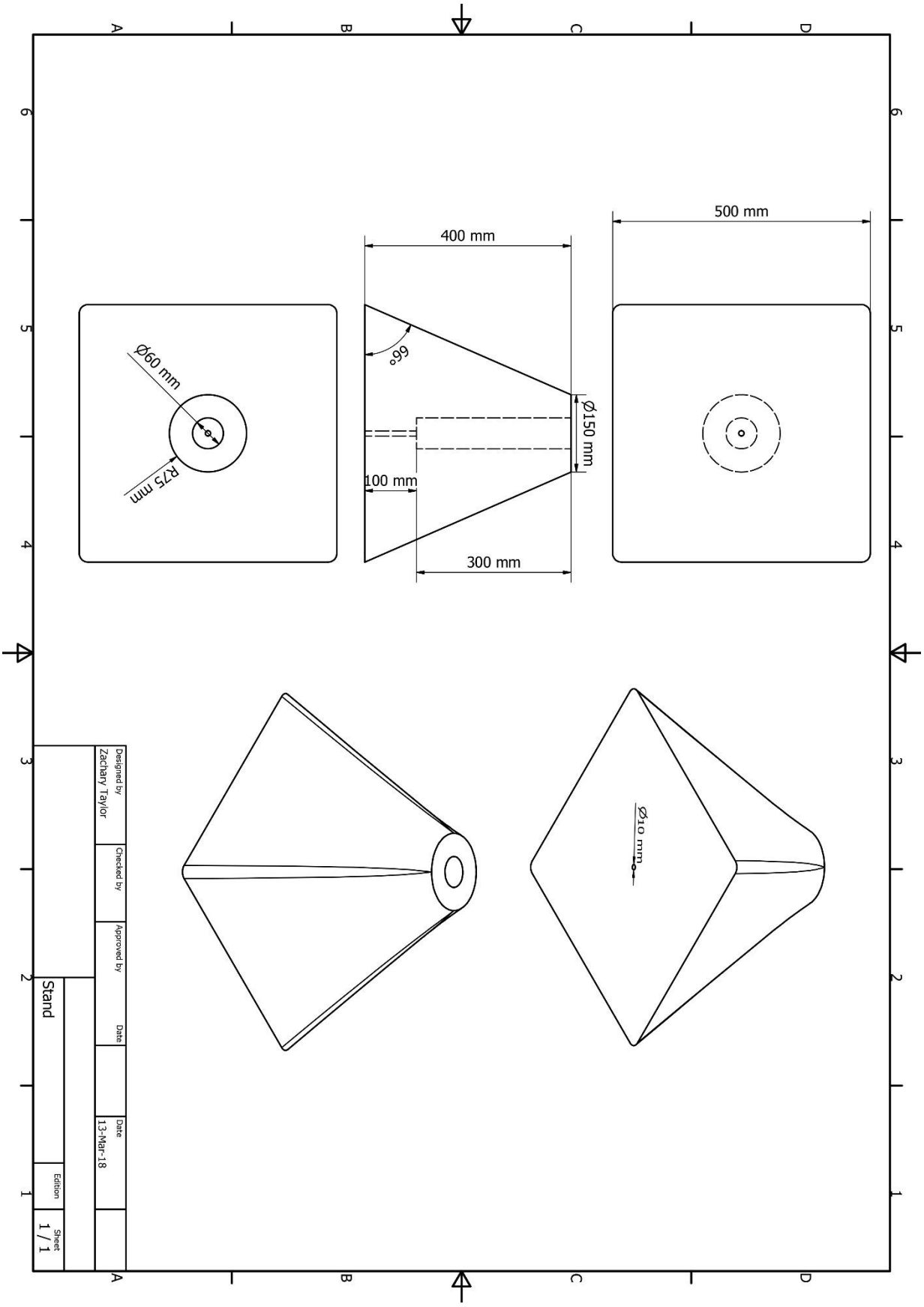

Drawing 23 - Stand

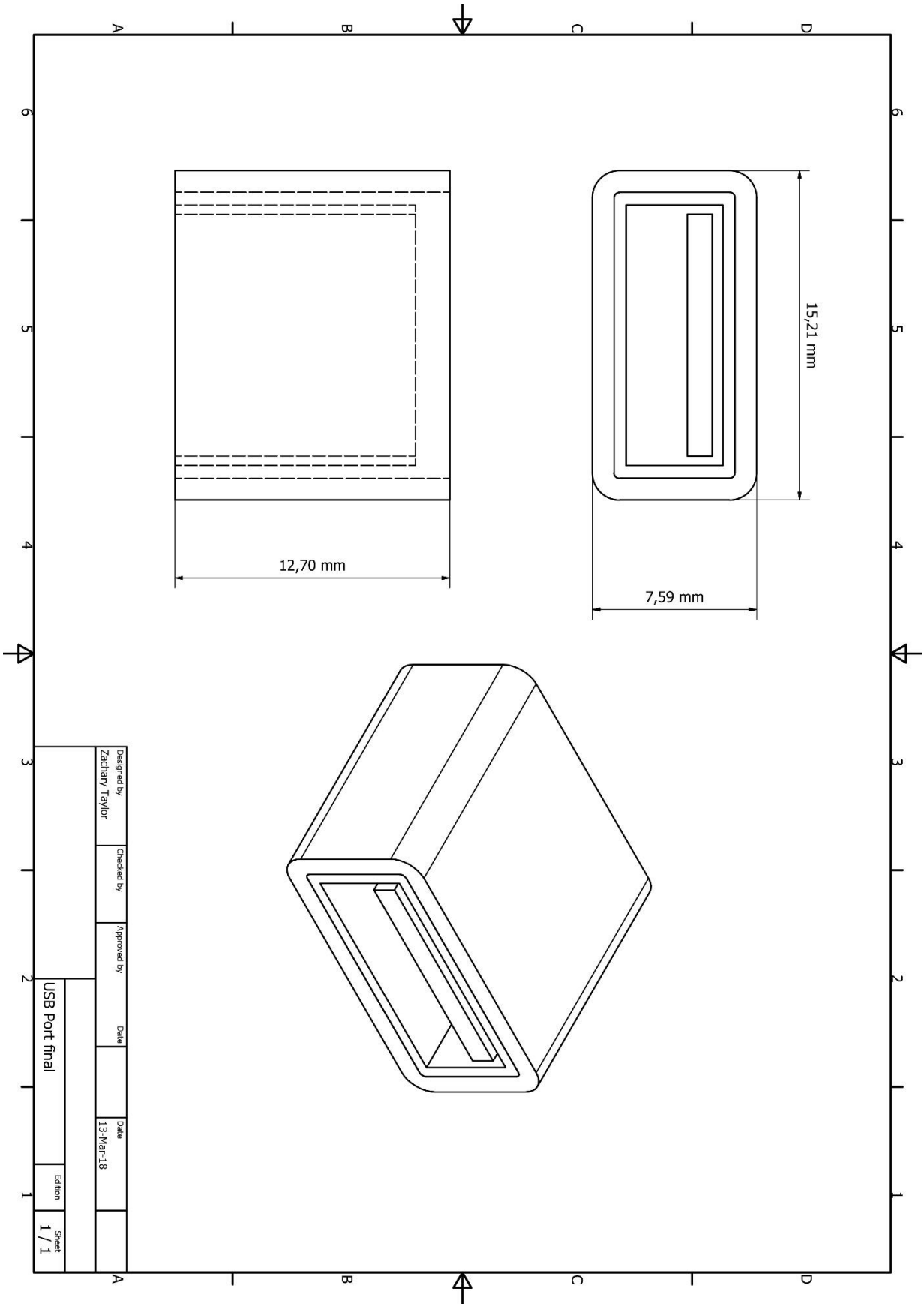

Drawing 24 - USB Port

Appendix 3. Circuit Diagrams

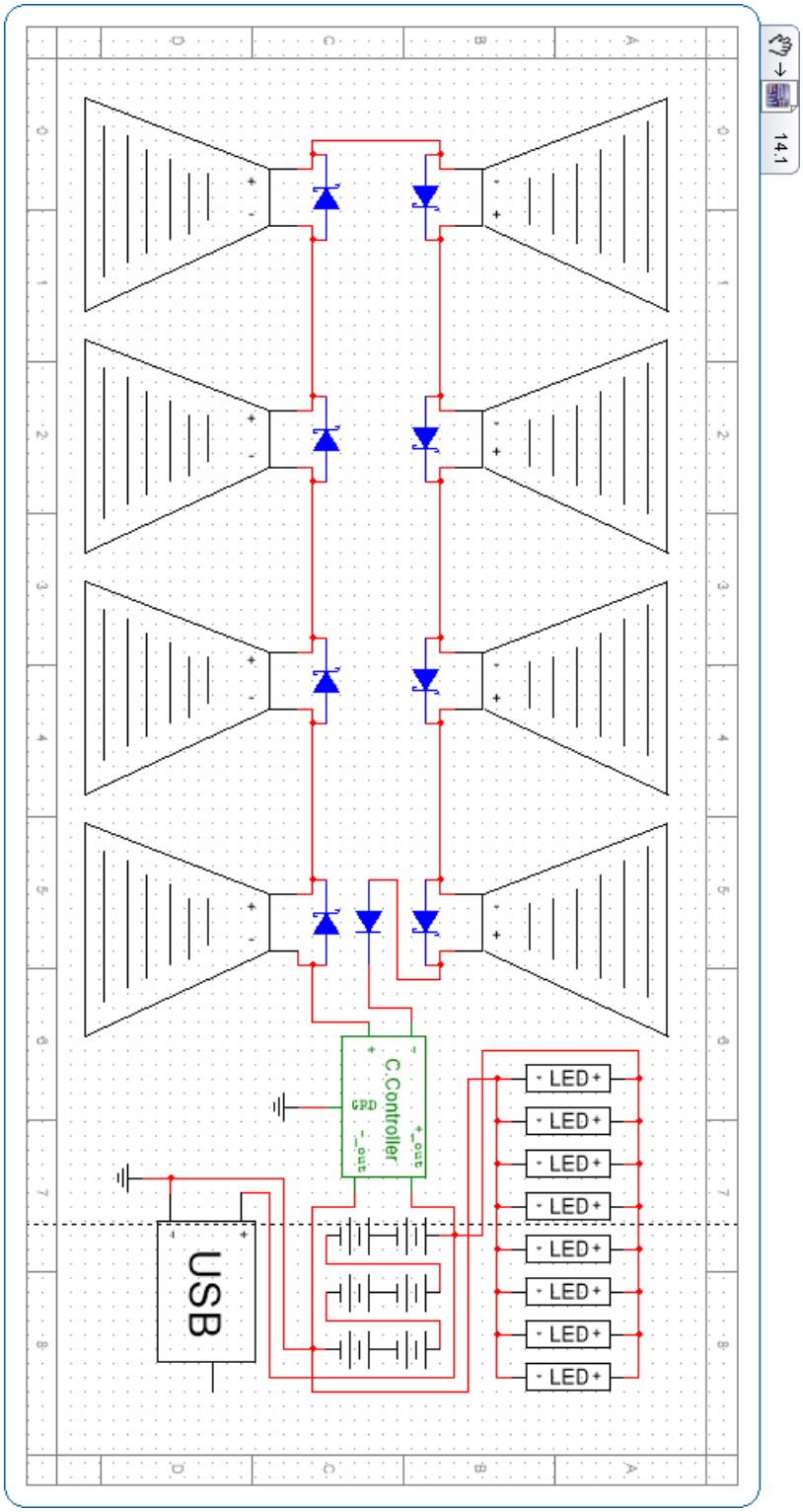

Drawing 25 - Main Circuit

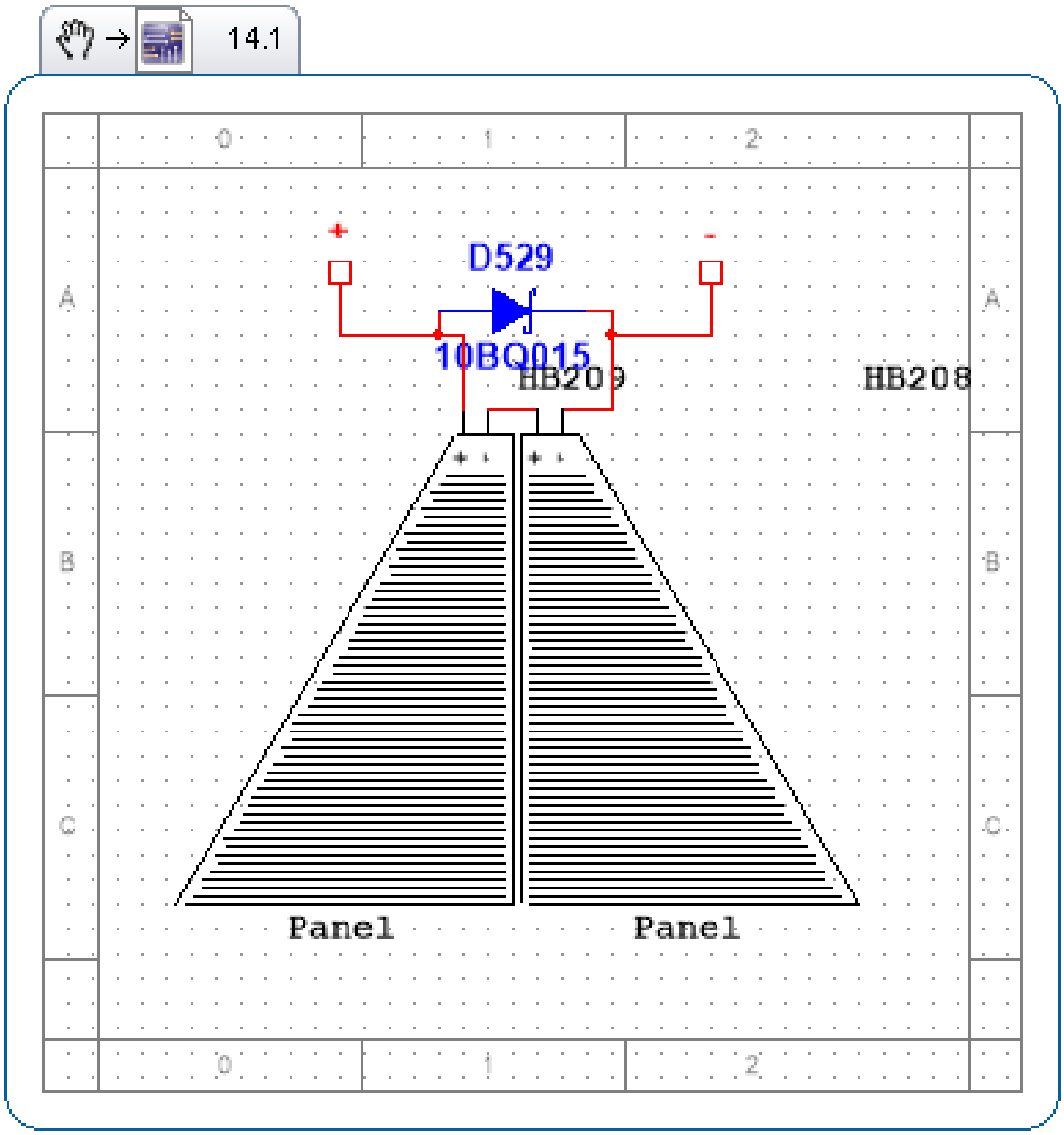

Drawing 26 - Panel Circuit

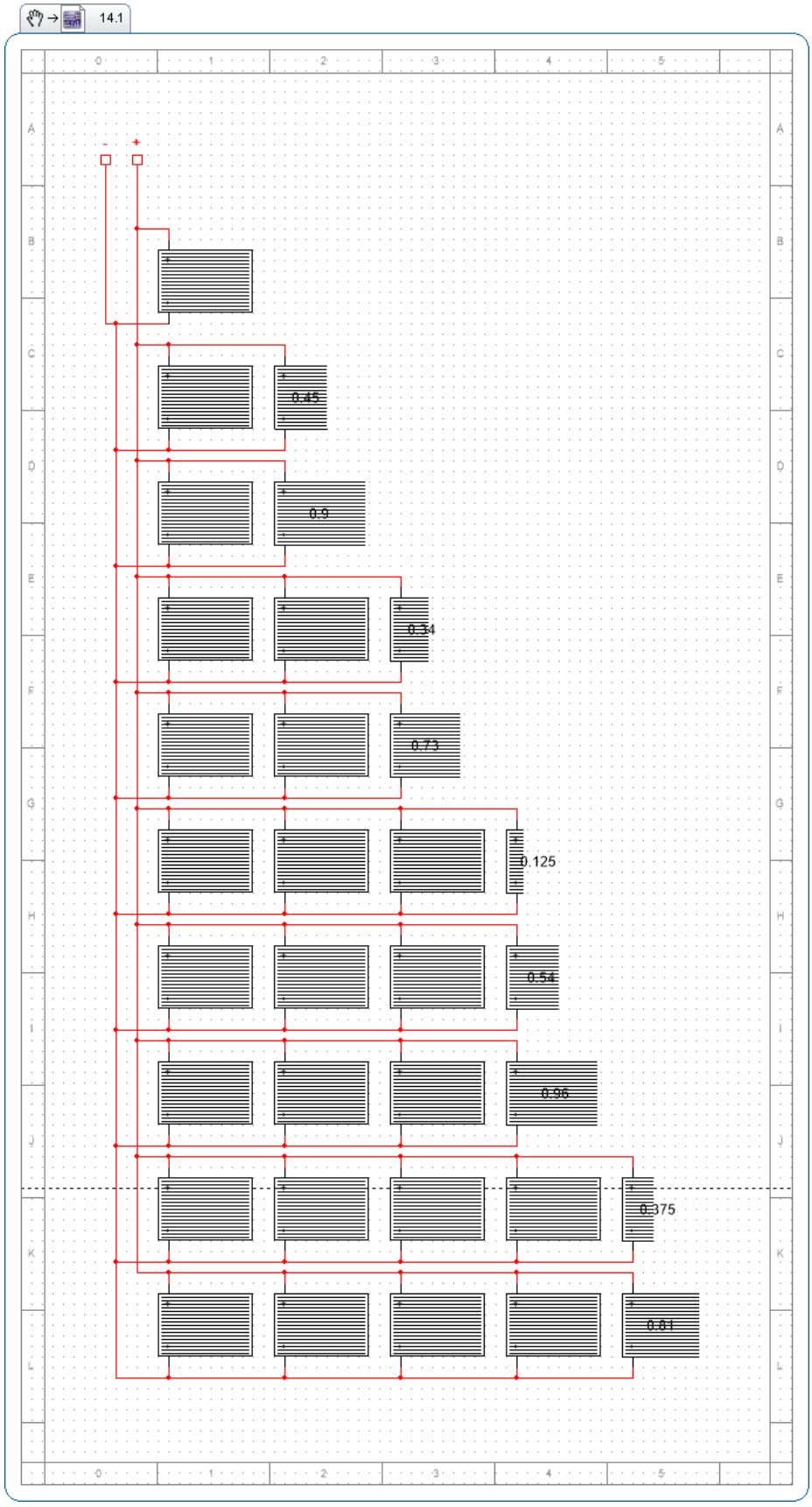

Drawing 27 - Panel Circuit

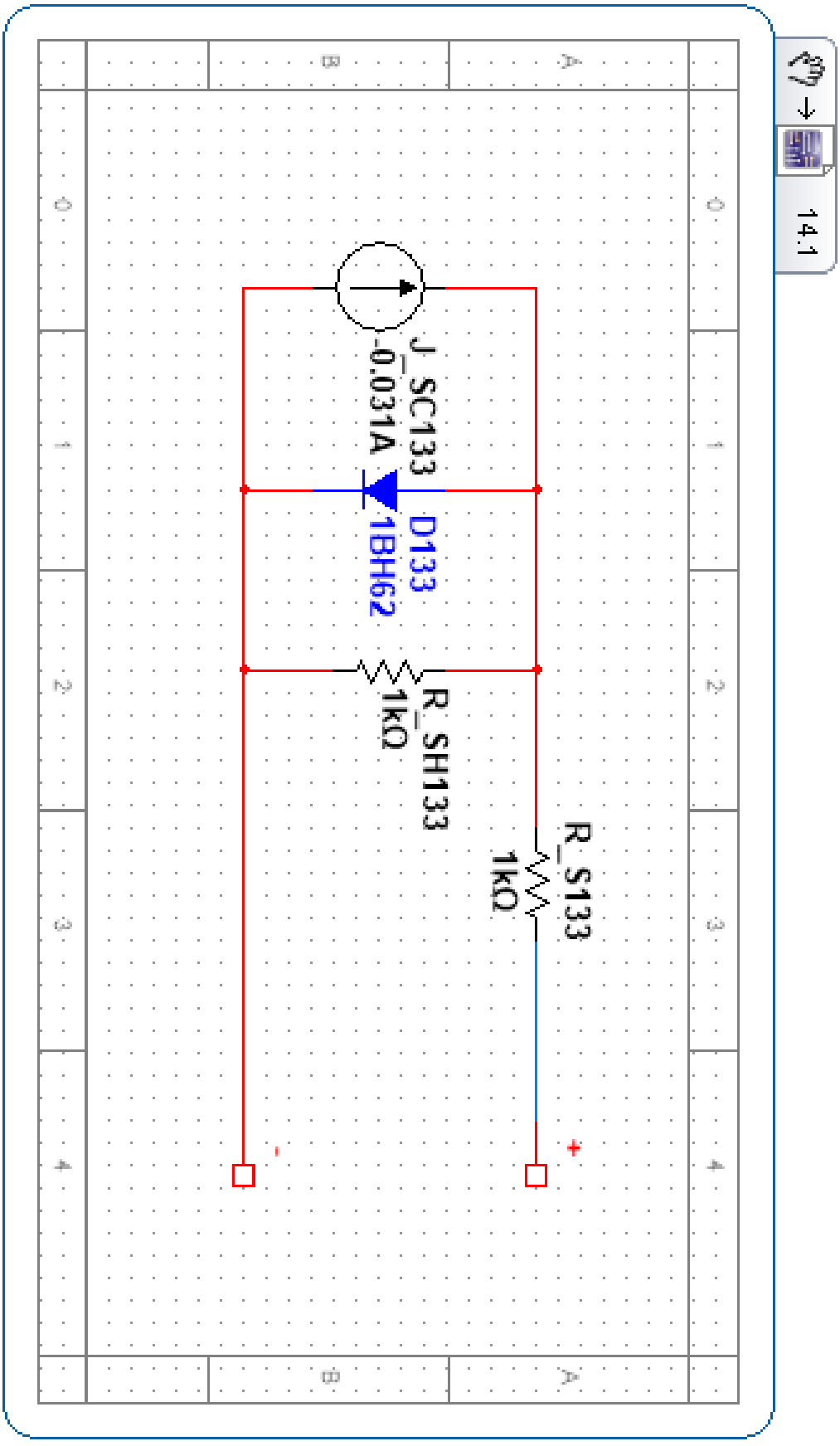

Drawing 28 - Base Circuit

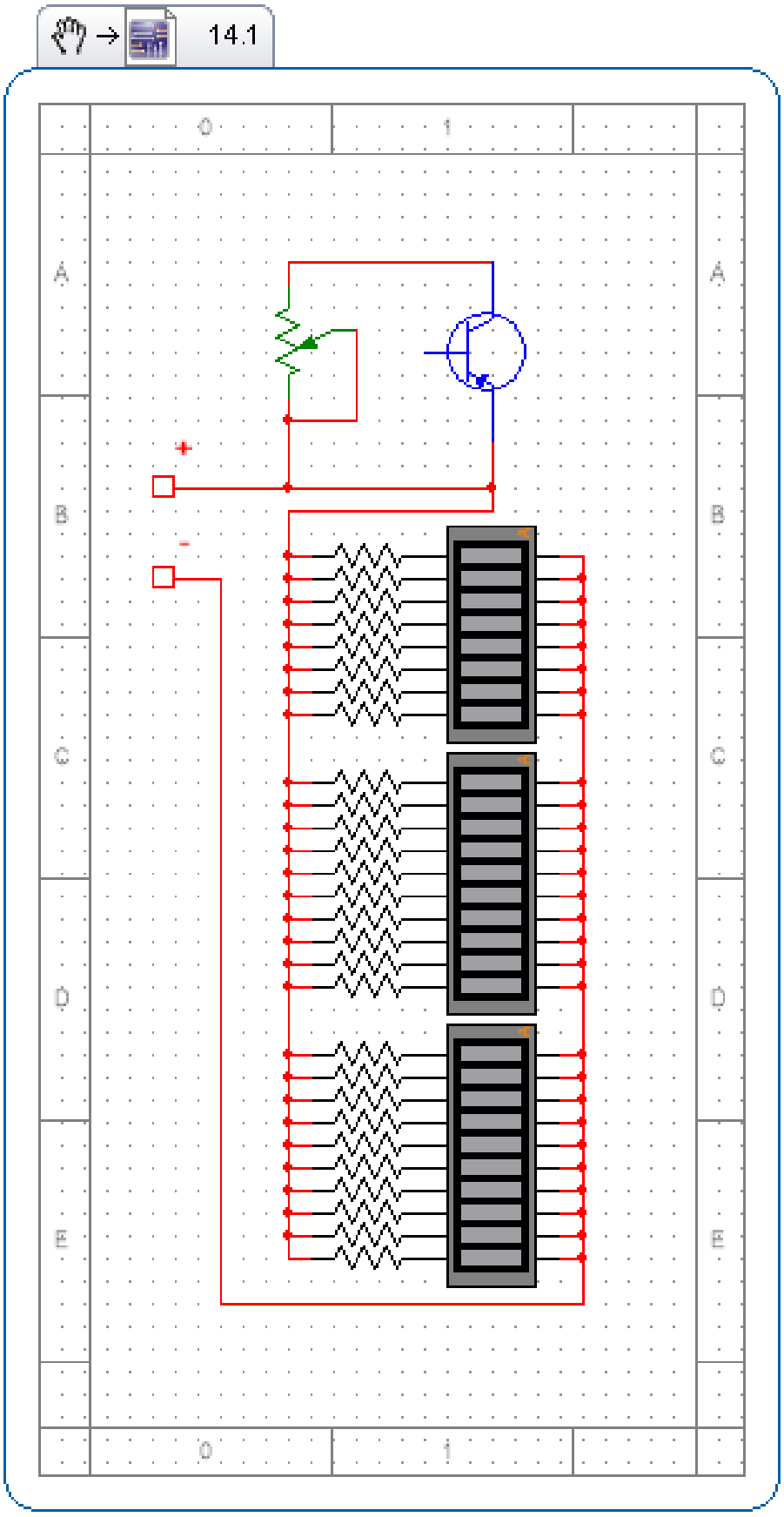

Drawing 29 - LED Circuit

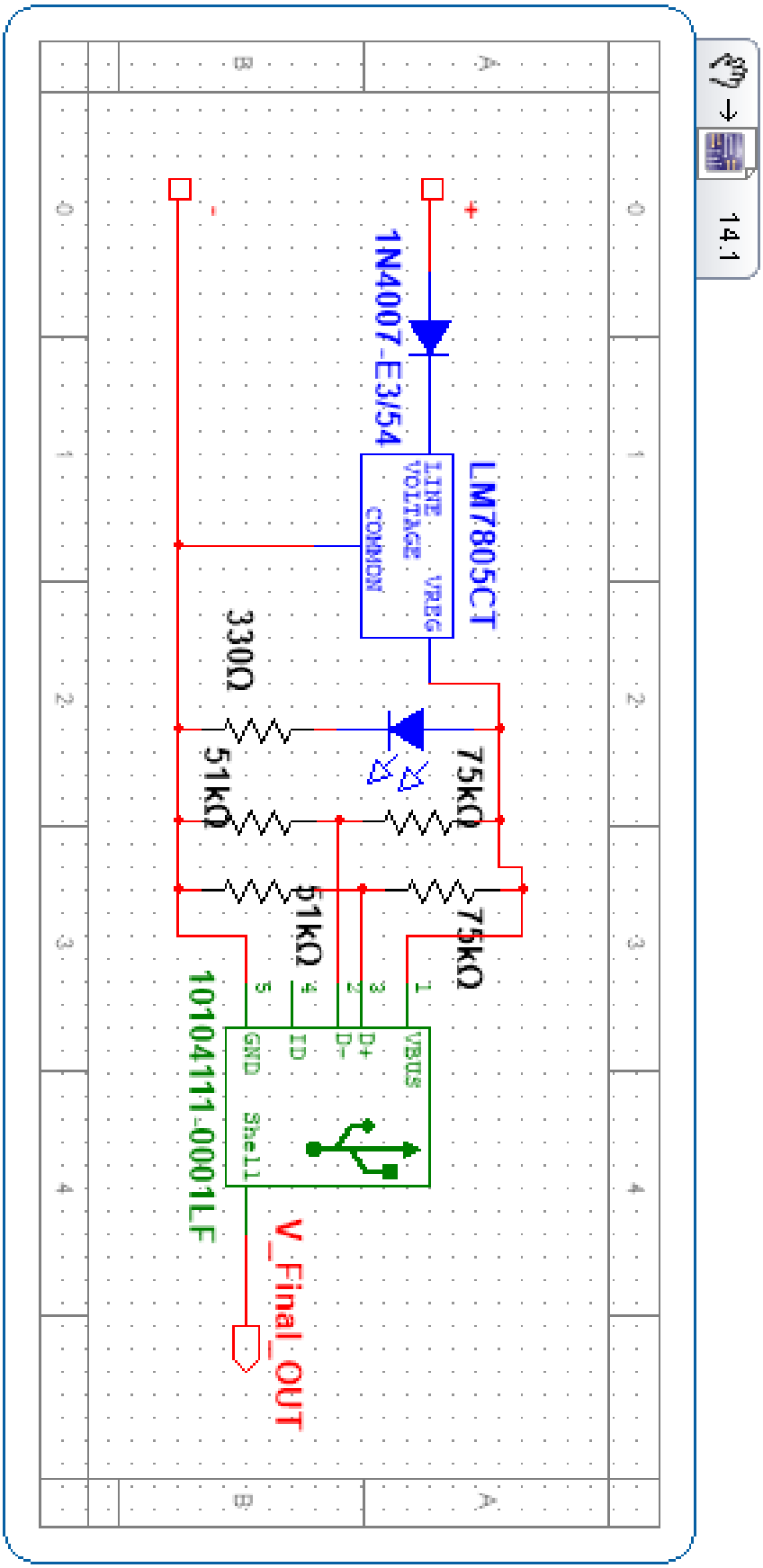

Drawing 30 - USB Circuit